Journal of Medicinal Chemistry

Article

Discovery of 4,5,6,7-Tetrahydrobenzo[1,2-d]thiazoles as Novel DNA Gyrase Inhibitors Targeting the ATP-Binding Site

Tihomir Tomasic, Sotirios Katsamakas, Ziga Hodnik, Janez Ilaš, Matjaz Brvar, Tom J Solmajer, Sofia Montalvao, Päivi Tammela, Mihailo Banjanac, Gabrijela Ergovic, Marko Anderluh, Lucija Peterlin Maši#, and Danijel Kikelj

J. Med. Chem., **Just Accepted Manuscript** • Publication Date (Web): 22 Jun 2015

Journal of Medicinal Chemistry is published by the American Chemical Society. 1155 Sixteenth Street N.W., Washington, DC 20036

Discovery of 4,5,6,7-Tetrahydrobenzo[1,2-*d*]thiazoles as Novel DNA Gyrase Inhibitors Targeting the ATP-Binding Site

Tihomir Tomašič,[a,‡] Sotirios Katsamakas,[a,b,‡] Žiga Hodnik,[a] Janez Ilaš,[a] Matjaž Brvar,[c] Tom Solmajer,[c] Sofia Montalvão,[d] Päivi Tammela,[d] Mihailo Banjanac,[e] Gabrijela Ergović,[e] Marko Anderluh,[a] Lucija Peterlin Mašič[a] and Danijel Kikelj[a,]*

[a]University of Ljubljana, Faculty of Pharmacy, Department of Medicinal Chemistry, Aškerčeva 7, 1000 Ljubljana, Slovenia

[b]Aristotle University of Thessaloniki, Faculty of Health Sciences, School of Pharmacy, Department of Pharmaceutical Chemistry, 54124 Thessaloniki, Greece

[c]National Institute of Chemistry, Laboratory for Biocomputing and Bioinformatics, Hajdrihova ulica 19, 1001 Ljubljana, Slovenia

[d]University of Helsinki, Faculty of Pharmacy, Centre for Drug Research, P.O. Box 56, FI-00014 Helsinki, Finland

[e]Galapagos Istrazivacki Ctr Doo, Prilaz Baruna Filipovica 29, HR-10000 Zagreb, Croatia

KEYWORDS antibacterial, DNA gyrase, docking, SPR, topoisomerase IV

ABSTRACT. Bacterial DNA gyrase and topoisomerase IV are essential enzymes that control the topological state of DNA during replication and validated antibacterial drug targets. Starting from a library of marine alkaloid oroidin analogs, we identified low micromolar inhibitors of *E. coli* DNA gyrase, based on the 5,6,7,8-tetrahydroquinazoline and 4,5,6,7-tetrahydrobenzo[1,2-*d*]thiazole scaffolds. Structure-based optimization of the initial hits resulted in low nanomolar *E. coli* DNA gyrase inhibitors, some of which exhibited micromolar inhibition of *E. coli* topoisomerase IV and of *S. aureus* homologs. Some of the compounds possessed modest antibacterial activity against Gram positive bacterial strains, while their evaluation against wild-type, *impA* and Δ*tolC E. coli* strains suggests that they are efflux pump substrates and/or do not possess the physico-chemical properties necessary for cell wall penetration. Our study provides a rationale for optimization of this class of compounds towards balanced dual DNA gyrase and topoisomerase IV inhibitors with antibacterial activity.

INTRODUCTION

The increasing emergence of pathogenic bacteria resistant to antibacterial drugs in both community- and hospital-acquired infections is a serious threat to global health, since currently available therapies will no longer be effective in treating these infections.[1] Although the rate of bacterial resistance to currently used antibacterials is on the rise, there have recently been only a few successful examples of new antibacterial drugs with novel modes of action entering the drug market.[2]

Bacterial topoisomerases are enzymes that catalyze changes in DNA topology and are clinically validated targets for antibacterial drug discovery.[3] Bacterial DNA gyrase and topoisomerase IV are type IIA topoisomerases that catalyze reactions involving the transient break of both strands of DNA.[4] Both enzymes modify the topological state of DNA, which is vital to DNA replication, repair and decatenation and is thus essential for cell viability. DNA gyrase is involved in negative supercoiling of DNA during replication, whereas topoisomerase IV is involved in the decatenation of daughter DNA following DNA replication. DNA gyrase is a heterotetrameric protein consisting of two GyrA and two GyrB subunits (A_2B_2), while topoisomerase IV is composed of two ParC and two ParE subunits (C_2E_2) that are homologous to GyrA and GyrB, respectively. The GyrA and ParC subunits are involved in DNA transit, while the GyrB and ParE subunits contain ATPase domains.[5]

The complexity of reactions in DNA replication catalyzed by DNA gyrase and topoisomerase IV offers multiple opportunities for therapeutic intervention. Both enzymes are targets of fluoroquinolones, a clinically important class of antibacterial drugs, which interact mostly with GyrA and ParC subunits and stabilize the enzyme-DNA complex,[6] and of aminocoumarins (e.g.

novobiocin and clorobiocin) that bind to GyrB and ParE.[7] Growing resistance to fluoroquinolones limits their therapeutic use[8] and therefore stimulates the search for new inhibitor classes that target different enzyme binding sites in order to avoid cross-resistance with the fluoroquinolones.

Due to the structural similarities between DNA gyrase and topoisomerase IV, dual targeting is possible in most bacteria, which prolongs the onset of resistance and makes bacterial type IIA topoisomerases attractive targets for discovering novel antibacterial drugs.[9] Their potential for dual targeting is one of the main reasons for several currently on-going drug discovery programs in the pharmaceutical industry.[10] For example, GyrB and dual targeting GyrB/ParE inhibitors have been identified among 5-(3-pyrazolyl)thiazoles,[11] azaindoles,[12] pyrrolo[2,3-*d*]pyrimidines,[13,14] imidazo[1,2-*a*]pyridine ureas,[15] benzimidazole ureas (Figure 1),[16] and pyrrolamides[17,18] (Figure 2a). Although these inhibitors target the ATP-binding site of GyrB and/or ParE, they usually display good selectivity profiles against eukaryotic ATP-binding proteins (e.g. kinases, human topoisomerase II).[19,20] Despite all the efforts to discover further GyrB or dual-targeting GyrB/ParE inhibitors, none have advanced into the clinic. Most of the GyrB/ParE inhibitors display potent MICs values against Gram positive bacteria. However, developing molecules with balanced dual-targeting activity that possess the physico-chemical property profiles necessary to result in potent antibacterial activity against Gram negative pathogens and to elude their multi-drug efflux pumps remains very challenging, since only few GyrB/ParE inhibitors possess cellular activity against Gram negative bacteria.[21]

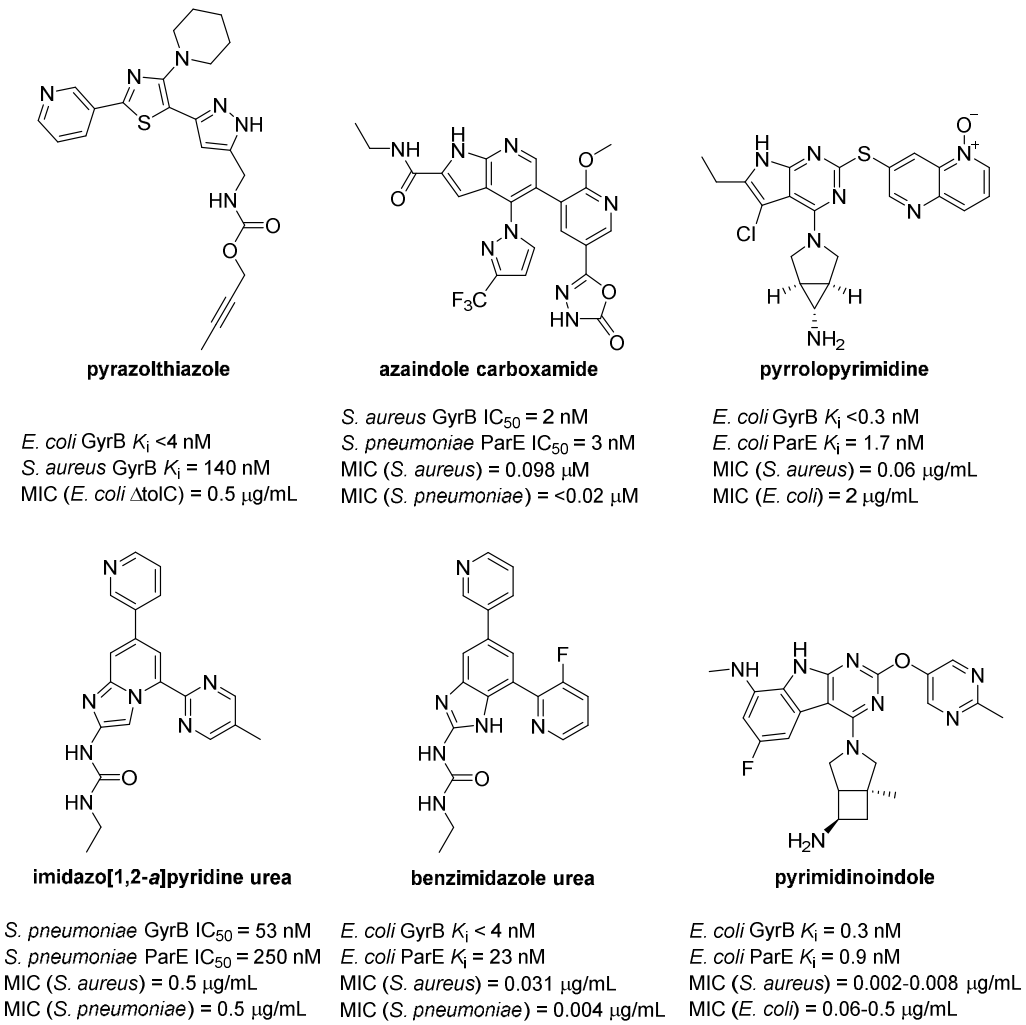

Figure 1. Examples of selected structural types of GyrB or dual-targeting GyrB/ParE inhibitors.

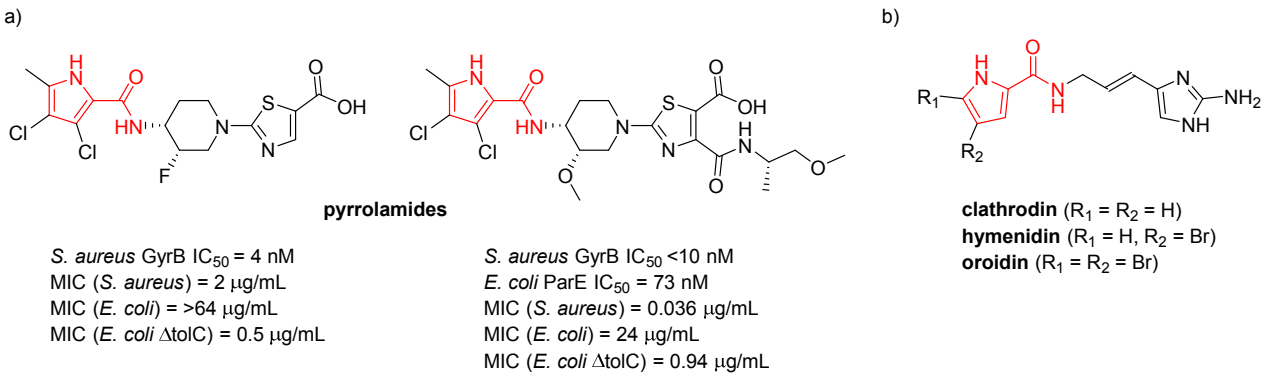

Figure 2. a) Pyrrolamide-based GyrB inhibitors and b) 2-aminoimidazole marine alkaloids clathrodin, hymenidin and oroidin possessing the pyrrolamide moiety (in red).

Recently, we have been involved in design and synthesis of several series of analogs of marine alkaloids clathrodin, oroidin and hymenidin (Figure 2b) displaying voltage-gated sodium channel modulatory activity,[22-25] antimicrobial activity,[26] inhibition of bacterial biofilm formation[27] and apoptosis inducing activity in HepG2 and THP-1 cell lines.[28] Some of these compounds incorporate a bromo substituted pyrrolamide moiety and are therefore structurally similar to the recently discovered pyrrolamide-based GyrB inhibitors[17,18] (Figure 2). This observation motivated us to test some of the synthesized clathrodin analogs for inhibition of DNA gyrase from *Escherichia coli*. Our library of 120 clathrodin analogs was enriched by structure-based virtual screening, using the *E. coli* GyrB crystal structure (PDB entry: 4DUH[29]), selecting the twenty top ranked compounds, and testing them for *E. coli* DNA gyrase inhibition. This resulted in three initial hits with IC_{50} values between 12 μM and 170 μM (compounds **1-3**, Figure 3). A common structural feature of hits **1-3** is the hydrophobic 4,5-dibromo-1*H*-pyrrole moiety, which suggested testing compounds **4** and **5** (Figure 3) that contain the smaller 4-bromo-1*H*-pyrrole and the bulkier 1*H*-indole moiety, respectively. Besides pyrrolamide moiety, the hydrophobic character of the substituents on the pyrrole ring appears to play a crucial role, since among compounds **3-5** 4,5-dibromo-1*H*-pyrrole-based **3** was found to be the most active, with an IC_{50} value of 12 μM, followed by the 1*H*-indole-based compound **5** (IC_{50} = 21 μM), while the 4-bromo-1*H*-pyrrole-based compound **4** possessed only weak activity (IC_{50} = 520 μM).

We describe here the structural optimization of these initial hits toward potent *E. coli* DNA gyrase inhibitors that also possess weak activity against *Staphylococcus aureus* DNA gyrase and *E. coli* and *S. aureus* topoisomerase IV. Molecular docking binding mode studies of inhibitors in the ATP-binding pocket of *E. coli* GyrB guided the selection of compounds for synthesis and provided a rationale for the observed structure-activity relationship (SAR). Evaluation of

antibacterial activity against Gram positive *S. aureus* and *Enterococcus faecalis* and Gram negative *E. coli* and *Pseudomonas aeruginosa* highlighted some compounds possessing modest antibacterial activity against Gram positive bacterial strains.

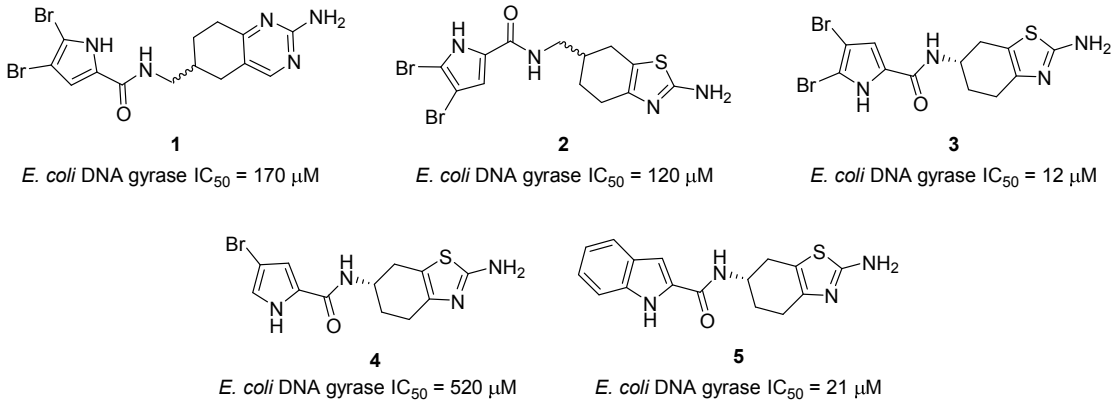

Figure 3. Oroidin analogs identified as *E. coli* DNA gyrase inhibitors.

RESULTS AND DISCUSSION

Design. Several crystal structures of GyrB-inhibitor complexes have been shown to reveal conserved binding modes of inhibitors in the GyrB ATP-binding site. Inhibitors partially mimic the binding of ATP by forming hydrogen bonds with Asp73 (*E. coli* GyrB numbering) and a structurally conserved water molecule, both of which are in contact with the adenine moiety of ATP.[30] Inhibitors thus usually possess adjacent hydrogen bond acceptor and donor groups (Figure 4a). Common structural features of inhibitors are also additional functionalities interacting with the Arg136 and/or Arg76 side chain.

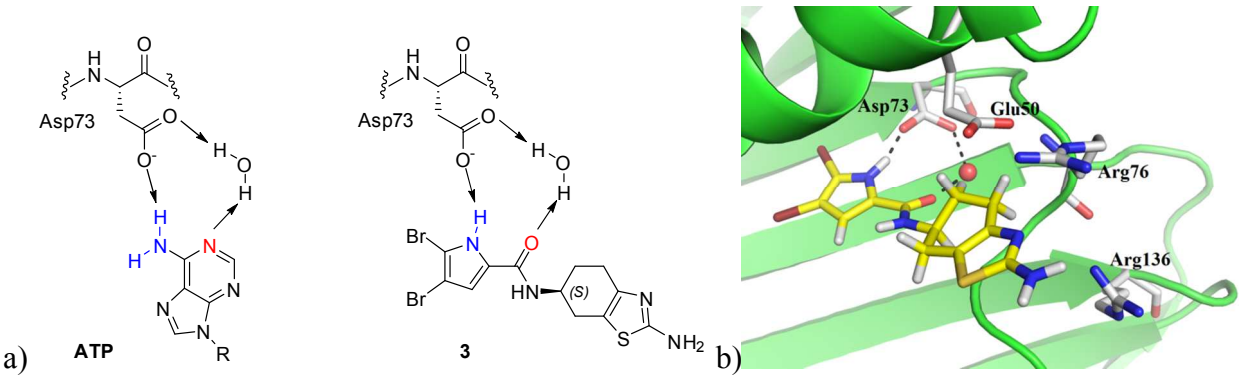

Figure 4. a) Schematic representation of the hydrogen bonding network between Asp73, the conserved water molecule and the adenine moiety of ATP (*left*) or the pyrrolamide moiety of compound **3** (*right*) in the *E. coli* GyrB ATP-binding site. b) The FlexX-predicted binding mode of compound **3** (in *yellow* sticks) in the ATP-binding site of *E. coli* GyrB (PDB entry: 4DUH[29]; in *green*). Hydrogen bonds are displayed as black dashed bonds. The figure was prepared by PyMOL.[31]

Preliminary data from the virtual screening hits showed that in the tetrahydrobenzothiazole series the additional methylene bridge between the carboxamide group and 2-amino-4,5,6,7-tetrahydrobenzo[1,2-*d*]thiazole scaffold had a negative effect on *E. coli* DNA gyrase inhibition (compounds **2** *vs* **3**). Consequently, the structures of compounds **3** and **5**, which were found to be the most active in the library of available oroidin analogs, and analog of compound **1** without the methylene bridge were optimized (Figure 5). In the calculated binding mode of compound **3** in the ATP-binding site of *E. coli* GyrB (PDB entry: 4DUH), the 4,5-dibromo-1*H*-pyrrole-2-carboxamide moiety is seen to be buried in the hydrophobic pocket and to form hydrogen bonds with the Asp73 side chain and the conserved water molecule, while the 2-amino group on the thiazole ring is positioned in such a way as to enable substitution with functional groups for interaction with Arg76 and/or Arg136 (Figure 4). The results of molecular docking calculations

indicated that the oxalyl, malonyl and succinyl moieties attached to the 2-amino group of the 5,6,7,8-tetrahydroquinazoline or 4,5,6,7-tetrahydrobenzo[1,2-*d*]thiazole cores are of such lengths as to enable the formation of hydrogen bond(s) with the Arg136 side chain. In addition, we have also investigated the effects of (*i*) replacing the 4,5-bromo-1*H*-pyrrole by the 4,5-dichloro-1*H*-pyrrole or 1*H*-indole moiety and (*ii*) chirality by preparing the *R* isomer of compound **3** (Figure 5).

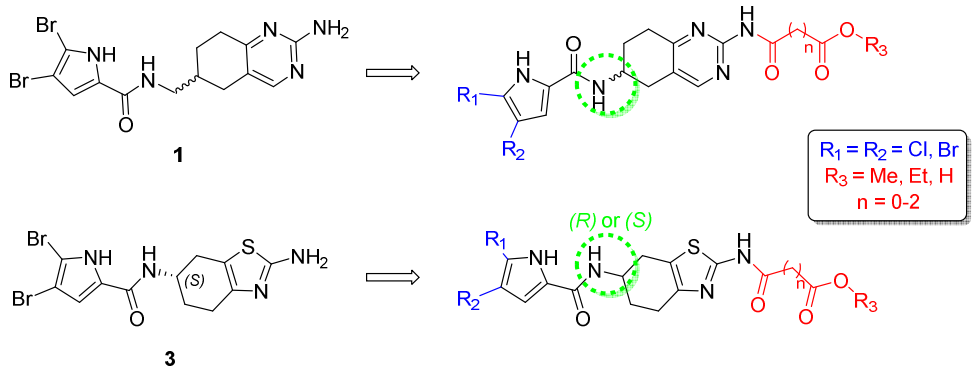

Figure 5. Design strategy for optimization of initial hits **1** and **3**.

Chemistry. The key intermediate **6** of the tetrahydroquinazoline series was synthesized as described by Marinko and co-workers.[32] 5,6,7,8-Tetrahydroquinazolines **7**, **8** and **9** were then synthesized by acylation of **6** with the corresponding 2,2,2-trichloro-1-(1*H*-pyrrol-2-yl)ethanones[33] in *N,N*-dimethylformamide (DMF), using Na_2CO_3 as base (Scheme 1). Analog **10** (Scheme 1) was synthesized with standard *O*-(benzotriazol-1-yl)-*N*,*N*,*N*′,*N*′-tetramethyluronium tetrafluoroborate (TBTU)-promoted coupling of **6** with the 1*H*-indole-2-carboxylic acid at room temperature.

With the aim to synthesize analogs **15** and **16**, which would significantly contribute to our envisaged SAR study, we acylated compounds **9** and **10** with methyl malonyl chloride in DMF to yield compounds **11** and **12** (Scheme 1). The subsequent attempt at methyl ester cleavage with 1 M sodium or lithium hydroxide in THF or methanol resulted in an unusual amide bond

cleavage at position 2 and consequential isolation of compounds **9** and **10**. Our further attempt to cleave the methyl ester of compounds **11** and **12** with lithium iodide in pyridine at reflux resulted in decarboxylation of these β-ketocarboxylic acids. Since such a lithium iodide-promoted decarboxylation has already been described,[34] we attempted the synthesis of benzyl-protected analogs **13** and **14** to give the desired analogs **15** and **16**. This was achieved by the TBTU-promoted coupling of compounds **9** and **10** with the 3-(benzyloxy)-3-oxopropanoic acid at 40 ºC (Scheme 1). Subsequent catalytic hydrogenation of compounds **13** and **14** again resulted in decarboxylation of the β-ketocarboxylic acid (e.g. compound **17**), which suggested that the desired acids **15** and **16** are not stable under the conditions used.

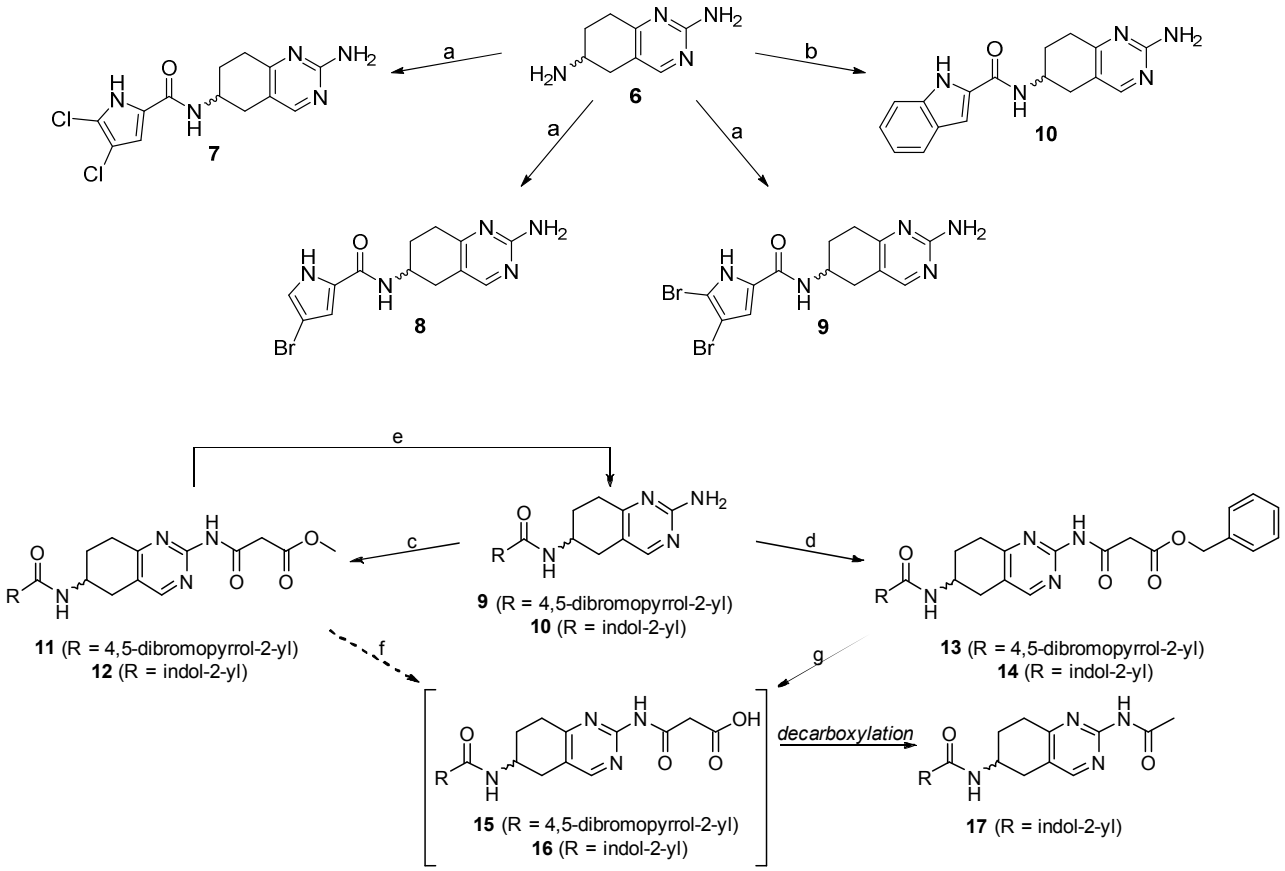

Scheme 1. Reagents and conditions: (*a*) for **7**: 2,2,2-trichloro-1-(4,5-dichloro-1*H*-pyrrol-2-yl)ethanone, for **8**: 2,2,2-trichloro-1-(4-bromo-1*H*-pyrrol-2-yl)ethanone, for **9**: 2,2,2-trichloro-1-(4,5-dibromo-1*H*-pyrrol-2-yl)ethanone, Na_2CO_3, DMF, 35 ºC, 2.5-3 h; (*b*) 1*H*-indole-2-

carboxylic acid, TBTU, Et_3N, DMF, r.t., 2.5 h; (*c*) methyl malonyl chloride, Et_3N, DMF, r.t., 17 h; (*d*) 3-(benzyloxy)-3-oxopropanoic acid, TBTU, Et_3N, DMF, 40 ºC, 4 h; (*e*) 1 M NaOH or LiOH, THF or MeOH, r.t. or 0 °C; (*f*) LiI, pyridine, reflux; (*g*) H_2, Pd/C, MeOH/THF, r.t., 3 h.

Racemic 4,5,6,7-tetrahydrobenzo[1,2-*d*]thiazol-2,6-diamine (**18**) was synthesized and optical resolution of the racemate to (*S*)-**18** and (*R*)-**18** enantiomers was performed as described by Schneider and Mierau.[35] In the X-ray structure of L-(+)-tartaric acid salt of (-)-**18** chiral center in position 6 was shown to have the *S* configuration.[35] Since specific rotations of (*S*)-**18** and (*R*)-**18** were in agreement with the values reported in the literature,[35] no additional experiments were performed to determine the configuration of the compounds. Synthesis of the (*S*)-4,5,6,7-tetrahydrobenzo[1,2-*d*]thiazol-2,6-diamines **3**, **4** and **22** was achieved by standard synthetic procedures by acylation of the (*S*)-4,5,6,7-tetrahydrobenzo[1,2-*d*]thiazole-2,6-diamine ((***S***)-**18**) with the 2,2,2-trichloro-1-(4,5-dibromo-1*H*-pyrrol-2-yl)ethanone, 2,2,2-trichloro-1-(4-bromo-1*H*-pyrrol-2-yl)ethanone or 2,2,2-trichloro-1-(4,5-dichloro-1*H*-pyrrol-2-yl)ethanone in DMF, respectively (Scheme 2).[22] TBTU-promoted coupling of (***S***)-**18** with 1*H*-indole-2-carboxylic acid, 5-fluoro-1*H*-indole-2-carboxylic acid or 5-chloro-1*H*-indole-2-carboxylic acid afforded compounds **5**, **20** and **21** (Scheme 2).

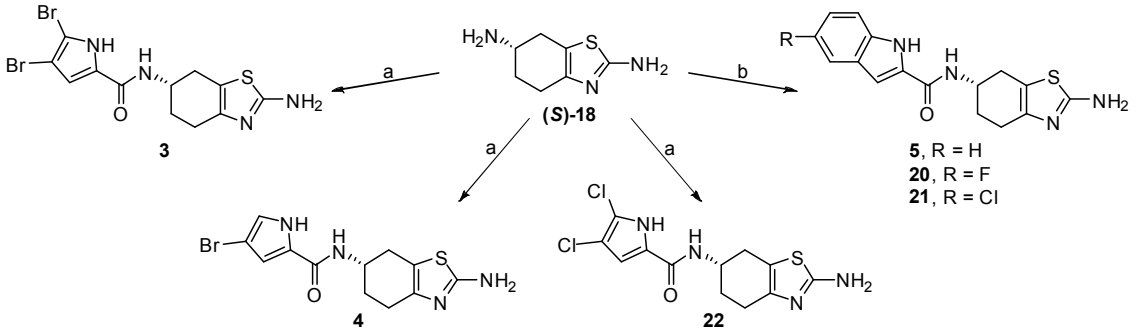

Scheme 2. Reagents and conditions: (*a*) for **3**: 2,2,2-trichloro-1-(4,5-dibromo-1*H*-pyrrol-2-yl)ethanone, for **4**: 2,2,2-trichloro-1-(4-bromo-1*H*-pyrrol-2-yl)ethanone, for **22**: 2,2,2-trichloro-1-

(4,5-dichloro-1*H*-pyrrol-2-yl)ethanone, Na_2CO_3, DMF, 35 ºC, 2-3 h; (*b*) for **5**: 1*H*-indole-2-carboxylic acid, for **20**: 5-fluoro-1*H*-indole-2-carboxylic acid, for **21**: 5-chloro-1*H*-indole-2-carboxylic acid, TBTU, Et_3N, DMF, r.t., 2.5 h.

According to the general scheme for structural optimization of the initial hit **3** (Figure 5) and of its 1*H*-indole-, 4-bromo-1*H*-pyrrole- and 4,5-dichloro-1*H*-pyrrole-based analogs **5**, **4** and **22**, the compounds were acylated at the amino group at position 2 of the (*S*)-4,5,6,7-tetrahydrobenzo[1,2-*d*]thiazole moiety with ethyl oxalyl chloride, methyl malonyl chloride or methyl succinyl chloride in 1,4-dioxane at room temperature (Scheme 3). The resulting products were 4,5-dibromo-1*H*-pyrrole-based esters **23-25**, 4-bromo-1*H*-pyrrole-based ester **27**, 1*H*-indole-based esters **28-30**, and 4,5-dichloro-1*H*-pyrrole-based esters **31-33**. Esters were hydrolyzed to their carboxylic acids **34-36** and **38-44** using alkaline conditions (Scheme 3). To further explore SAR, *R*-isomers **19**, **26** and **37** were prepared using the same conditions as described for the synthesis of their *S* enantiomers **3**, **24** and **35**, starting from (***R***)**-18** (Scheme 3). To evaluate the importance of the terminal carboxyl group of compound **35** for DNA gyrase inhibition, *N*-acetyl compound **45** was prepared from **3** using acetyl chloride and triethylamine in 1,4-dioxane. Furthermore, compound **3** was also converted to the dihydropyrimidone analog **46** using one-pot cyclization with acryloyl chloride, sodium carbonate and sodium iodide in acetonitrile.[36] Carboxamide **47** was prepared by aminolysis of the methyl ester **24**, by bubbling gaseous ammonia into solution of **24** in ethanol, with the aim of improving penetration of compounds **24** and **35** through the membrane into the cytoplasm of bacteria.

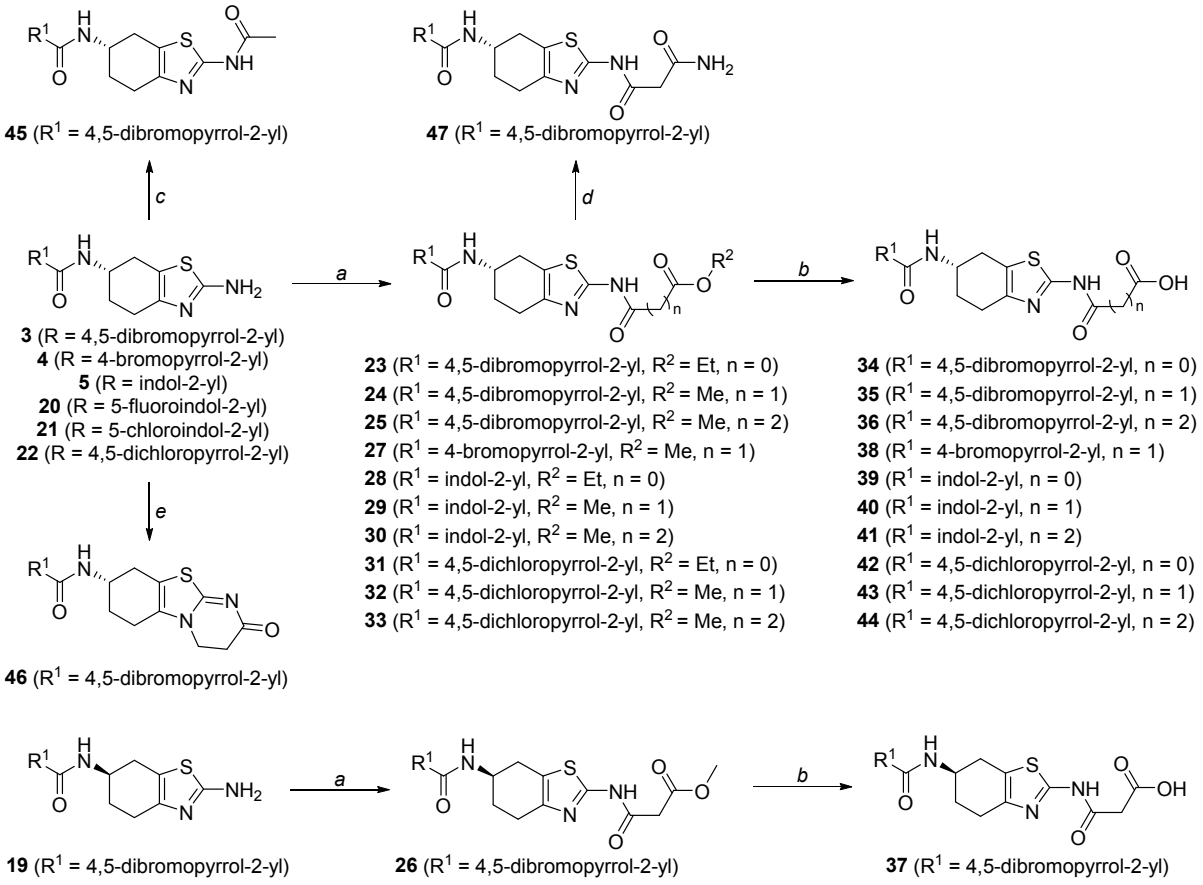

Scheme 3. Reagents and conditions: (*a*) ethyl oxalyl chloride (for **23**, **28** and **31**) or methyl malonyl chloride (for **24**, **26-28** and **32**) or methyl succinyl chloride (for **25**, **30** and **33**), Et_3N, 1,4-dioxane, r.t., 24 h; (*b*) 1 M NaOH, MeOH/H_2O, r.t., 24 h; (*c*) acetyl chloride, Et_3N, 1,4-dioxane, r.t., 24 h; (*d*) $NH_{3(g)}$, EtOH, r.t., 2 h; (*e*) acryloyl chloride, Na_2CO_3, CH_3CN, 0 °C, 2 h, then NaI, 80 °C, 24 h.

***In vitro* Enzyme Inhibition.** All synthesized compounds were tested for *E. coli* DNA gyrase inhibitory activity, using the DNA gyrase supercoiling assay. Those that inhibited *E. coli* DNA gyrase with IC_{50} values below 50 μM were also tested for inhibition of *S. aureus* DNA gyrase, as well as topoisomerases IV from *E. coli* and *S. aureus* using the topoisomerase IV relaxation

assay (Tables 1-4). Results are presented as residual activities (RA) of the enzyme at 100 μM of the tested compound or IC_{50} values for the more active compounds (RA < 50% at 100 μM).

Inhibitory activities of the 5,6,7,8-tetrahydroquinazoline-2,6-diamines **7-12** and **17** are presented in Table 1. Compound **9**, an analog of the initial hit **1** (IC_{50} = 170 μM) but lacking the methylene bridge, displayed, as expected, improved *E. coli* DNA gyrase inhibition, with an IC_{50} value of 2.9 μM, since similar difference in activity between compounds with and without the methylene bridge was also observed in the case of the 4,5,6,7-tetrahydrobenzo[1,2-*d*]thiazole-2-amines **2** and **3**. Replacing the 4,5-dibromo-1*H*-pyrrole moiety of **9** by 4-bromo-1*H*-pyrrole (**8**, IC_{50} = 35 μM), 1*H*-indole (**10**, IC_{50} = 29 μM) or 4,5-dichloro-1*H*-pyrrole (**7**, IC_{50} = 5.7 μM) resulted in weaker activity. Contrary to expectations, introduction of the malonyl group on the 2-amino group of the 5,6,7,8-tetrahydroquinazoline-2,6-diamine scaffold of **9** and **10** did not result in improved *E. coli* DNA gyrase inhibition. *N*-Methylmalonyl-4,5-dibromo-1*H*-pyrrole-based compound **11** (IC_{50} = 2.6 μM) possessed inhibitory activity similar to that of its *N* non-substituted analog **9** (**(**IC_{50} = 2.9 μM), while the indole-based compound **12** (RA = 77% at 100 μM) was devoid of this activity. Since, because of their instability due to decarboxylation, our attempts to prepare carboxylic acid derivatives **15** and **16** were unsuccessful, only the decarboxylated acetylated compound **17** was tested and found to possess weak activity (RA = 52% at 100 μM).

The weak antibacterial activity of these inhibitors (see below) prompted us to test them also against *E. coli* topoisomerase IV as well as against *S. aureus* DNA gyrase and topoisomerase IV. Compounds **7-11**, that displayed inhibition of *E. coli* DNA gyrase with IC_{50} values between 2.6 μM and 35 μM, were found to be inactive at 100 μM in all three assays.

Table 1. Inhibition of *Escherichia coli* and *Staphylococcus aureus* DNA gyrase and topoisomerase IV by the 5,6,7,8-tetrahydroquinazolines **7-12** and **17**.

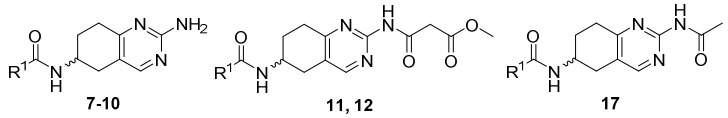

cpd	R^1	DNA gyrase IC_{50} [μM] or RA [%][a]		topoisomerase IV IC_{50} [μM] or RA [%][a]		*E. coli* MIC [μg/mL]		
		E. coli	*S. aureus*	*E. coli*	*S. aureus*	wt	*tolC*	*impA*
neg[b]	-	100%	100%	100%	100%	-	-	-
NB[c]	-	0.17 μM	0.040 μM	11 μM	27 μM	-	-	-
7	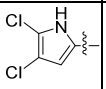	5.7 μM	90%	96%	106%	n.t.[d]	n.t.	n.t.
8	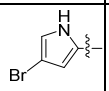	35 μM	100%	97%	105%	n.t.	n.t.	n.t.
9	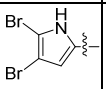	2.9 μM	96%	102%	98%	>256	>256	>256
10	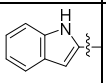	29 μM	119%	97%	103%	n.t.	n.t.	n.t.
11	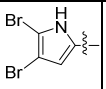	2.6 μM	71%	97%	98%	>256	64	256
12	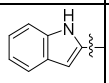	77%	n.t.	n.t.	n.t.	n.t.	n.t.	n.t.
17	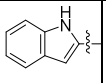	52%	n.t.	n.t.	n.t.	n.t.	n.t.	n.t.

[a]Residual activity of the enzyme at 100 μM of the tested compound.

[b]1% DMSO was used as a negative control.

[c]NB – novobiocin was used as a positive control.

[d] n.t. – not tested.

Comparison of the *E. coli* DNA gyrase inhibitory activities of hits **3** and **4** (Table 2) revealed that substituents on the pyrrole ring have an important effect on inhibition. Bromine atoms presumably form hydrophobic interactions in the hydrophobic pocket of the ATP-binding site. In addition, they increase the acidity of the pyrrole amino group, thereby increasing the strength of the hydrogen bond formed with the Asp73 side chain. This explains why the dibromo-substituted pyrrole-based compound **3** (IC_{50} = 12 μM) exhibited more potent DNA gyrase inhibition than its monobromopyrrole counterpart **4** (IC_{50} = 520 μM) (Table 2). According to the calculated binding mode of **3** in the ATP-binding site of *E. coli* DNA gyrase (Figure 4), there is sufficient space for introduction of a hydrogen bond acceptor on the 2-amino group of the thiazole moiety for interaction with the guanidine group of Arg136. Indeed esters **23**, **24** and **25**, containing the oxalyl, malonyl and succinyl groups, displayed improved *E. coli* DNA gyrase inhibition with IC_{50} values of 0.10 μM, 0.096 μM and 0.093 μM, suggesting their interaction with Arg136. The possibility of hydrogen bond formation between the carbonyl oxygens of these moieties with the guanidine group of Arg136 is clearly indicated in the docking experiments (Figure 7). Carboxylic acid derivatives **34-36** with IC_{50} values between 0.049 μM and 0.069 μM were not substantially more potent *E. coli* DNA gyrase inhibitors than their ester counterparts with IC_{50} values between 0.093 μM and 0.10 μM. Their comparable activities indicate that the terminal ester or acid groups of compounds **23-25** and **34-36** probably form a hydrogen bond, and not an ionic/salt bridge interaction, with the guanidine group of Arg136. Alternatively, the carboxylic acid could form a salt bridge with Arg136, but there is a higher desolvation penalty for taking the carboxylate from the aqueous environment to the enzyme binding site than for esters, which could explain comparable IC_{50} values of carboxylic acids and esters. Another hydrogen bond

partner in the guanidine-carboxylate interaction in the enzyme environment could be a neighboring water molecule. A hydrogen bond interaction with Arg76 (Fig. 7b) could also be responsible for the similar binding strengths of ester and carboxylic acid derivatives.

The SAR was further explored by preparing *R* isomers **19**, **26** and **37** of compounds **3**, **24** and **35**. The non-substituted compound **19** (IC_{50} = 47 μM) exhibited 4-fold weaker activity than its *S* isomer **3** (IC_{50} = 12 μM). Changing the stereochemistry from *S* to *R* had an even more pronounced effect in the cases of ester **26** (IC_{50} = 9.1 μM *vs* 0.096 μM for **24**) and carboxylic acid **37** (IC_{50} = 0.50 μM *vs* 0.069 μM for **35**). Consequently, a conclusion can be made that in the investigated series, *S* isomers are more potent inhibitors than the *R* optical antipodes.

Since the introduction of the *N*-malonyl moiety (**24** and **35** *vs* **3**) had a positive effect on binding affinity, we also prepared *N*-malonyl compounds **27** (IC_{50} = 25 μM) and **38** (IC_{50} = 14 μM) that bear the 4-bromo-1*H*-pyrrole moiety. Their activity was greater than that of **4** (IC_{50} = 520 μM) but 200-fold lower from the dibromo counterparts **24** and **35**. This again highlights the importance for potent inhibition of the bromo substituents on the pyrrole ring, since the pyrrolamide moiety is buried deep in the ATP-binding site and forms crucial hydrogen bonds and hydrophobic interactions with the protein.

The importance of the terminal ester or carboxylic group of compounds **23-27** and **34-38** was assessed by preparing the *N*-acetyl derivative **45**, which displayed *E. coli* DNA gyrase inhibition with an IC_{50} value of 0.15 μM, which is 3-fold weaker than that observed for the most potent compound **36** (IC_{50} = 0.049 μM) but 80-fold more potent than that of the parent compound **3** (IC_{50} = 12 μM) implying that the acetyl carbonyl group of **45** is, importantly, most probably involved in hydrogen bond formation. In contrast, cyclization of **3** to the dihydropyrimidone derivative **46** (IC_{50} = 12 μM) did not result in improved inhibition.

The amide derivative **47**, prepared from ester **24** (IC_{50} = 0.096 μM), in an attempt to improve the penetration through the membrane of bacteria into the cytoplasm (see below), displayed decreased activity (IC_{50} = 1.7 μM) as compared to its ester counterpart.

E. coli DNA gyrase inhibitors (IC_{50} < 50 μM) bearing the bromo-substituted pyrrole moiety were also tested for their inhibition of *E. coli* topoisomerase IV (Table 2). They were found to be mostly inactive or only weak inhibitors (IC_{50} values between 73 μM and 200 μM for compounds **24**, **34** and **35**). The common structural feature of these active compounds is the presence of the oxalyl or malonyl moiety. A similar trend was observed when these inhibitors were tested for inhibition of *S. aureus* DNA gyrase and topoisomerase IV (IC_{50} values between 76 μM and 270 μM for compounds **23**, **24**, **34**, **35**, **36** and **45**) (Table 2), which probably explains their weak antibacterial activity against some Gram positive pathogens (see below).

Table 2. Inhibition of *Escherichia coli* and *Staphylococcus aureus* DNA gyrase and topoisomerase IV by the 4,5,6,7-tetrahydrobenzo[1,2-*d*]thiazoles containing the 4,5-dibromo-1*H*-pyrrole (**3**, **19**, **23-26**, **34-37**, **45-47**) or 4-bromo-1*H*-pyrrole moiety (**4**, **27**, **38**).

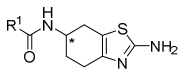

3, 4, 19

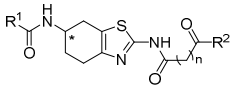

23-27, 34-38, 47

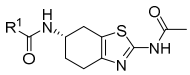

45

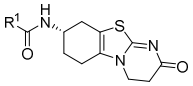

46

cpd	*	R^1	R^2	n	DNA gyrase IC_{50} (K_d[a]) [μM] or RA [%][b]		topoisomerase IV IC_{50} [μM] or RA [%][b]		*E. coli* MIC [μg/mL]		
					E. coli	*S. aureus*	*E. coli*	*S. aureus*	wt	*tolC*	*impA*
neg[c]	-	-	-	-	100%	100%	100%	100%	-	-	-
NB[d]	-	-	-	-	0.17 μM	0.040 μM	11 μM	27 μM	-	-	-
3	*S*	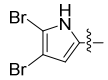	-	-	12 μM (3 μM[a])	90%	101%	102%	>256	64	64

4	*S*	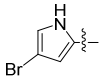	-	-	520 μM	n.t.[ec]	n.t.	n.t.	n.t.	n.t.	n.t.
19	*R*	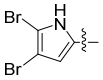	-	-	47 μM	118%	96%	92%	>256	64	64
23	*S*	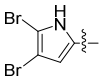	OEt	0	0.10 μM	80 μM	74%	180 μM	>256	128	>256
24	*S*	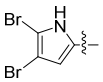	OMe	1	0.096 μM (0.072 μM[a])	110 μM	86 μM	74%	>256	16	32
25	*S*	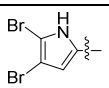	OMe	2	0.093 μM (0.15 μM[a])	113%	97%	99%	>256	32	64
26	*R*	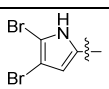	OMe	1	9.1 μM	64%	101%	85%	>256	64	256
27	*S*	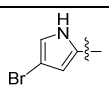	OMe	1	25 μM	100%	95%	104%	n.t.	n.t.	n.t.
34	*S*	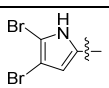	OH	0	0.058 μM	120 μM	200 μM	78 μM	>256	256	>256
35	*S*	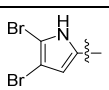	OH	1	0.069 μM (0.042 μM[a])	86 μM	74 μM	76 μM	>256	>256	>256
36	*S*	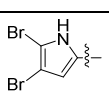	OH	2	0.049 μM (0.010 μM[a])	270 μM	90%	110 μM	>256	256	>256
37	*R*	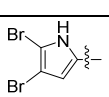	OH	1	0.50 μM	108%	96%	102%	>256	>256	>256
38	*S*	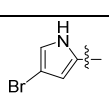	OH	1	14 μM	110%	96%	97%	n.t.	n.t.	n.t.
45	*S*	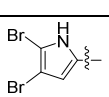	-	-	0.15 μM	26 μM	98%	101%	n.t.	n.t.	n.t.
46	*S*	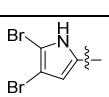	-	-	12 μM	n.t.	n.t.	n.t.	>256	>256	>256
47	*S*	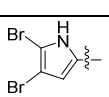	NH_2	1	1.7 μM	71%	97%	98%	>256	128	>256

[a] K_d as determined by surface plasmon resonance (see below).

[b]Residual activity of the enzyme at 100 μM concentration of the tested compound.

[c]1% DMSO was used as a negative control.

[d]NB – novobiocin was used as a positive control.

[e]n.t. – not tested.

Structural optimization of the indole-based initial screening hit **5** was less successful, the *E. coli* DNA gyrase inhibitory activities remaining in the micromolar range (Table 3). First, we explored whether additional substitution of the indole moiety at position 5 is tolerated by the enzyme active site. Introduction of a 5-fluoro or 5-chloro substituent was detrimental to the activity, with 5-fluoro-1*H*-indole **20** (IC_{50} = 270 μM) and 5-chloro-1*H*-indole **21** (RA = 94%) displaying weaker inhibition than **5** (IC_{50} = 21 μM). Following the optimization strategy described for bromopyrroles, we synthesized the indole-based oxalyl, malonyl and succinyl esters **28-30** and carboxylic acids **39-41**. These inhibited *E. coli* DNA gyrase with IC_{50} values between 7.6 μM and 35 μM, not significantly better than that of **5** (IC_{50} = 21 μM), so SAR of these series was not further explored. Indole-based compounds were also found to be devoid of activity against *E. coli* topoisomerase IV and *S. aureus* homologs (Table 3).

Table 3. Inhibition of *Escherichia coli* and *Staphylococcus aureus* DNA gyrase and topoisomerase IV by the 4,5,6,7-tetrahydrobenzo[1,2-*d*]thiazoles containing the 1*H*-indole moiety (**5**, **20, 21, 28-30**, **39-41**).

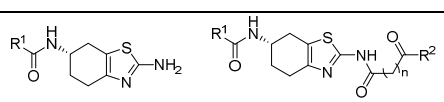

5, 20, 21 **28-30, 39-41**

cpd	R^1	R^2	n	DNA gyrase	topoisomerase IV	*E. coli* MIC

				IC_{50} [μM] or RA [%][a]		IC_{50} [μM] or RA [%][a]		[μg/mL]		
				E. coli	*S. aureus*	*E. coli*	*S. aureus*	wt	*tolC*	*impA*
neg[b]	-	-	-	100%	100%	100%	100%	-	-	-
NB[c]	-	-	-	0.17 μM	0.040 μM	11 μM	27 μM	-	-	-
5	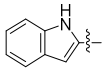	-	-	21 μM	87%	103%	100%	n.t.[d]	n.t.	n.t.
20	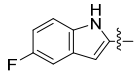	-	-	270 μM	n.t.	n.t.	n.t.	>256	>256	>256
21	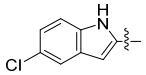	-	-	94%	n.t.	n.t.	n.t.	n.t.	n.t.	n.t.
28	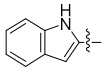	OEt	0	10 μM	76%	101%	99%	n.t.	n.t.	n.t.
29	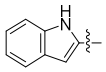	OMe	1	35 μM	n.t.	n.t.	n.t.	>256	>256	>256
30	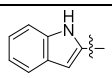	OMe	2	9.1 μM	87%	101%	104%	n.t.	n.t.	n.t.
39	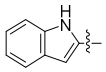	OH	0	7.7 μM	79%	47%	99%	>256	>256	128
40	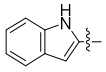	OH	1	7.6 μM	117%	96%	103%	>256	>256	>256
41	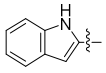	OH	2	8.1 μM	95%	99%	79%	>256	>256	>256

[a]Residual activity of the enzyme at 100 μM of the tested compound.

[b]1% DMSO was used as a negative control.

[c]NB – novobiocin was used as a positive control.

[d]n.t. – not tested.

Finally, we replaced the 4,5-dibromo-1*H*-pyrrole moiety of **3**, **23-25** and **34-36** by the 4,5-dichloro-1*H*-pyrrole moiety (compounds **22, 31-33**, **42-44**, Table 4). The chlorine analogs displayed less potent inhibition of *E. coli* DNA gyrase than their 4,5-dibromo-1*H*-pyrrole counterparts (Table 4), with malonyl acid **43** (IC_{50} = 0.13 μM) being the most potent. The

inhibition of *S. aureus* DNA gyrase and *E. coli* and *S. aureus* topoisomerase IV by dichloropyrroles **22**, **31-33** and **42-44** followed the trends observed in the other two series, with weaker activities in the micromolar range (IC_{50} values between 10 μM and 320 μM) as compared to inhibition of *E. coli* DNA gyrase.

Table 4. Inhibition of *Escherichia coli* and *Staphylococcus aureus* DNA gyrase and topoisomerase IV by the 4,5,6,7-tetrahydrobenzo[1,2-*d*]thiazoles containing the 4,5-dichloro-1*H*-pyrrole moiety (**22**, **31-33**, **42-44**).

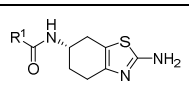

22

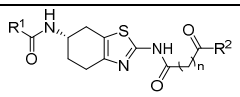

31-33, 42-44

cpd	R^1	R^2	n	DNA gyrase IC_{50} (K_d[a]) [μM] or RA [%][b]		topoisomerase IV IC_{50} [μM] or RA [%][b]		*E. coli* MIC [μg/mL]		
				E. coli	*S. aureus*	*E. coli*	*S. aureus*	wt	*tolC*	*impA*
neg[c]	-	-	-	100%	100%	100%	100%	-	-	-
NB[d]	-	-	-	0.17 μM	0.040 μM	11 μM	27 μM	-	-	-
22	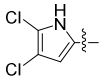	-	-	12 μM	85%	97%	98%	>256	64	64
31	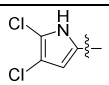	OEt	0	0.40 μM	320 μM	300 μM	290 μM	>256	256	>256
32	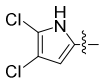	OMe	1	0.40 μM (0.050 μM[a])	63%	97%	101%	>256	32	32
33	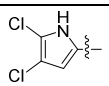	OMe	2	0.89 μM	86%	100%	93%	>256	>256	>256
42	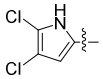	OH	0	0.59 μM	300 μM	82%	170 μM	>256	>256	>256
43	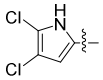	OH	1	0.13 μM (0.049 μM[a])	87%	98%	102%	>256	>256	>256

44	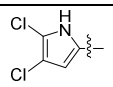	OH	2	0.30 μM	10 μM	72%	97%	>256	>256	>256

[a] K_d as determined by surface plasmon resonance (see below).

[b] Residual activity of the enzyme at 100 μM of the tested compound.

[c] 1% DMSO was used as a negative control.

[d] NB – novobiocin was used as a positive control.

Superposition of the crystal structures of DNA gyrase and topoisomerase IV from *S. aureus* and *E. coli* (Figure 6) provides a possible explanation for the observed differences in inhibition of these enzymes. The hydrophobic pocket of the ATP-binding site, that is predicted to bind the pyrrolamide moiety of inhibitors, is smaller in *S. aureus* GyrB and *E. coli* ParE than in *E. coli* GyrB or *S. aureus* ParE. For example, Val43, Met95 and Val167 in *E. coli* DNA gyrase are replaced by the larger Ile51, Leu103 and Ile175 in *S. aureus* DNA gyrase (Figure 6). As expected from the overlay of crystal structures, according to measurement by POVME[37] (**PO**cket **V**olume **ME**asurer) the pocket volume of *E. coli* GyrB (V = 157 Å^3) is larger than that of *S. aureus* GyrB (V = 140 Å^3), *E. coli* ParE (V = 149 Å^3) and *S. aureus* ParE (V = 155 Å^3). When these pocket volumes are compared with those of the 1*H*-indole-2-carboxamide (V = 143 Å^3), 4,5-dibromo-1*H*-pyrrole-2-carboxamide (V = 135 Å^3) and 4,5-dichloro-1*H*-pyrrole-2-carboxamide (V = 126 Å^3) (calculated by the Molinspiration property calculation service, www.molinspiration.com), these moieties can be accommodated in the *E. coli* DNA gyrase ATP-binding site but are probably too large to fit the smaller hydrophobic pocket of *S. aureus* DNA gyrase. A similar calculation can explain the weaker *E. coli* DNA gyrase inhibition by **20** and **21** than that by **5**, since the volumes of 5-fluoro-1*H*-indole-2-carboxamide (in **20**) and 5-chloro-1*H*-indole-2-carboxamide (in **21**) moieties are 148 Å^3 and 156 Å^3, being too bulky even for the larger hydrophobic pocket of *E. coli* DNA gyrase. An alternative explanation for the lower

activities in the case of *S. aureus* DNA gyrase could be the loss of a favorable interaction with Arg144 (Arg136 in *E. coli* GyrB, Fig. 7f).

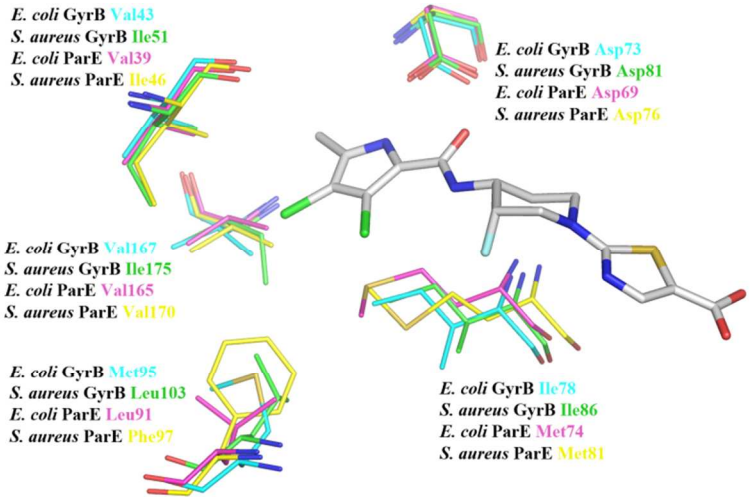

Figure 6. Overlay of crystal structures of GyrB from *E. coli* (PDB entry: 4DUH,[29] *in cyan*) and *S. aureus* (PDB entry: 3TTZ,[17] *in green*), ParE from *E. coli* (PDB entry: 4HZ0,[13] *in magenta*) and *S. aureus* (PDB entry: 4URL,[38] *in yellow*). Pyrrolamide-based GyrB inhibitor from the crystal structure 3TTZ is represented in grey sticks. For clarity, only less conserved residues defining the hydrophobic pocket of GyrB and ParE ATP-binding sites are shown, except for Asp, which is well conserved among various bacterial strains. Figure was prepared by PyMOL.[31]

***E.coli* DNA Gyrase ATPase Assay.** Compounds **3**, **23**, **34**, **40** and **43** were also tested for inhibition of *E. coli* DNA gyrase ATPase activity in a linked assay, which follows the hydrolysis of ATP via the conversion of NADH to NAD+, to provide further experimental evidence on their binding to the ATP-binding pocket of the enzyme. Results presented in Table 5 show between 2.1- and 8.3-fold weaker activities as those determined in the supercoiling assay. However, the ATPase assay SAR, although with a limited number of compounds tested, follows the SAR observed in the supercoiling assay, which further suggests the binding of 4,5,6,7-

tetrahydrobenzo[1,2-*d*]thiazoles **3**, **23**, **34**, **40** and **43** and their analogs to the ATP-binding site of DNA gyrase.

Table 5. Inhibition of the *Escherichia coli* DNA gyrase ATPase activity by the 4,5,6,7-tetrahydrobenzo[1,2-*d*]thiazoles **3**, **23**, **34**, **40** and **44**.

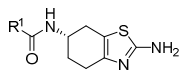

3

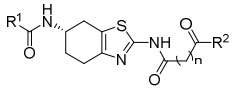

23, 34, 40, 43

cpd	R^1	R^2	n	*E. coli* DNA gyrase IC_{50} [μM]	
				supercoiling assay	ATPase assay
NB[a]	-	-	-	0.17 μM	0.13 μM
3	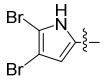	-	-	12 μM	25 μM
23	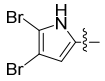	Et	0	0.10 μM	0.57 μM
34	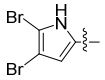	OH	0	0.058 μM	0.48 μM
40	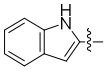	OH	1	7.6 μM	22 μM
43	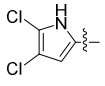	OH	1	0.13 μM	0.66 μM

[a]NB – novobiocin was used as a positive control.

Surface Plasmon Resonance (SPR) Experiments. The ability of inhibitors **3**, **24**, **25**, **32**, **35**, **36** and **43** to inhibit *E. coli* DNA gyrase *in vitro* was further evaluated by surface plasmon resonance. In contrast to the functional DNA gyrase assay that was used for screening and determining of IC_{50} values and comprises GyrA and GyrB subunits of DNA gyrase, the smaller

24 kDa N-terminal part of the GyrB subunit (GyrB24) was used for SPR experiments. The GyrB24 protein, immobilized on the CM5 chip, was used for testing using novobiocin as a standard. Inhibitors were tested at eight concentrations in three parallels, depending on the response of the immobilized protein. K_d values were calculated using Origin software with a steady state affinity binding model that assumes one site binding. The results revealed fast and tight binding of inhibitors **3**, **24**, **25**, **32**, **35**, **36** and **43** to the GyrB24 protein with K_d values in agreement with the previously determined IC_{50} values in the functional DNA gyrase assay. Measured K_d values for compounds **3**, **24**, **25**, **32**, **35**, **36** and **43** were 3.0 μM, 0.072 μM, 0.15 μM, 0.050 μM, 0.042 μM, 0.010 μM and 0.049 μM, which are consistent with their IC_{50} values of 12 μM, 0.096 μM, 0.093 μM, 0.40 μM, 0.069 μM, 0.049 μM and 0.13 μM (Tables 2 and 4), suggesting the binding of these pyrrolamide-based inhibitors to the ATP-binding site of *E. coli* DNA gyrase.

Antibacterial Activity. All prepared compounds that inhibited *E. coli* DNA gyrase were first screened for their antibacterial activity at 50 μM against two Gram negative (*Escherichia coli* ATCC 25922, *Pseudomonas aeruginosa* ATCC 27853) and two Gram positive (*Enterococcus faecalis* ATCC 29212, *Staphylococcus aureus* ATCC 25923) bacterial strains. Despite potent *E. coli* DNA gyrase inhibition, all compounds were found to be inactive against both Gram negative strains (Supplementary Figure S1). There are several possible explanations for the absence of antibacterial activity against *E. coli* and *P. aeruginosa.* Achieving antibacterial activity against Gram negative bacteria is challenging, since molecules have to be able to penetrate the cell envelope and, in addition, to avoid excretion by the efflux pumps. Firstly, the absence of the antibacterial activity can be attributed to excessive polarity of the compounds, responsible for poor permeability across the cell wall. Secondly, it has been claimed that sub-nanomolar activity

is required to generate sufficient antibacterial potency on Gram negative strains.[19] To assess whether our inhibitors are substrates of the efflux pumps and/or have permeability problems, we evaluated the compounds against permeabilized (*impA*) and efflux pump knockout (*ΔtolC*) strains of *E. coli* as well as the wild-type strain (Tables 1-4). In general, it appears that the *E. coli* DNA gyrase inhibitors presented in Tables 1-4 are substrates of the efflux pump tolC and/or possess unfavorable physico-chemical properties, since MIC values against *ΔtolC* and *impA E. coli* strains are lower for some compounds than for the wild-type *E. coli* strain. In detail, non-substituted compounds **3**, **19** and **22** (IC_{50} values between 12 μM and 47 μM) displayed weak, but still stronger antibacterial activity against *ΔtolC* and *impA E. coli* strains with MICs of 64 μg/mL than against the wild-type strain. Oxalyl, malonyl and succinyl acids **34-37** and **42-44** were devoid of antibacterial activity against *ΔtolC* and *impA* strains of *E. coli*, despite their potent *E. coli* DNA gyrase inhibition (IC_{50} values between 0.049 μM and 0.59 μM), while their ester analogs **23-25**, **31** and **32** (IC_{50} values between 0.093 μM and 0.40 μM) showed stronger antibacterial activities, with MICs between 16 μg/mL and 256 μg/mL. Compounds **24**, **25** and **32**, that exhibited MICs against *ΔtolC E. coli* strain below 32 μg/mL, were among the most potent *E. coli* DNA gyrase inhibitors in the series.

The antibacterial activities of compounds **3-5**, **7-12**, **17** and **19-47** against Gram positive *S. aureus* and *E. faecalis* were surprisingly weak at 50 μM, with growth inhibition less than 50% for the majority of compounds (Supplementary Figure S1). The only exceptions were compounds **24** (84.4% growth inhibition of *E. faecalis*), **25** and **32** (52.3% and 54.3% growth inhibition of *S. aureus*). Confirmatory dose-response experiments showed that MICs for these compounds were >125 μM (highest concentration tested). Therefore, their mode of action has not been determined. In view of their weak antibacterial activity against Gram positive strains

the compounds were also tested against *S. aureus* DNA gyrase and topoisomerase IV (described above, Tables 1-4). Since the compounds inhibited *S. aureus* enzymes in the micromolar range, if at all, this probably explains the absence of growth inhibition of Gram positive bacteria by these compounds. Indeed, in *S. aureus* strains IC_{50} values of less than 50 μM against the *S. aureus* GyrB are needed to result in MICs below 64 μg/mL.[39]

Molecular Modeling. Pyrrolamide-based DNA gyrase inhibitors, such as natural products clorobiocin[40] and kibdelomycin[38] and synthetic compounds[17,18] (Figure 2a) have been shown by X-ray crystallography to bind to the ATP-binding sites of DNA gyrase and topoisomerase IV. Since our oroidin-derived DNA gyrase inhibitors also contain the pyrrole-2-carboxamide moiety and showed binding affinity for GyrB subunit of *E. coli* DNA gyrase in the SPR experiment, one could anticipate that they bind to the ATP-binding site of the enzyme. Therefore, the binding of designed DNA gyrase inhibitors was studied by docking in the ATP-binding site of *E. coli* GyrB (PDB entry: 4DUH), using FlexX[41,42] as available in LeadIT[43] (BioSolveIT GmbH). The docking protocol was first validated by redocking of the inhibitor from the crystal structure in the defined binding site. The use of FlexX reproduced the experimentally determined inhibitor conformation with an all heavy atom root-mean square distance (RMSD) of 1.2 Å, which makes this software suitable for predicting binding modes of the novel DNA gyrase inhibitors and rationalization of the observed SAR.

Docking experiments predicted similar binding modes of 4,5-dibromo-1*H*-pyrroles, 1*H*-indoles and 4,5-dichloro-1*H*-pyrroles. A hydrogen bonding network was in all cases formed between the pyrrole-2-carboxamide or indole-2-carboxamide moiety of inhibitors, Asp73 side chain and the highly conserved structural water, while in some cases additional interactions were formed with Arg76 and/or Arg136 (Figure 7). For example, the potent *E. coli* DNA gyrase

inhibitor **23** (IC_{50} = 0.10 μM) and its carboxylic acid derivative **34** (IC_{50} = 0.058 μM) are predicted to form hydrogen bonds with Arg76 and Arg136 (Figure 7a and 7b). Both the carbonyl of the aminocarbonyl group at position 2 and the ester group of **23** appear to be in contact with the protein. This observation was confirmed with *N*-acetyl derivative **45** (IC_{50} = 0.15 μM), which showed more potent *E. coli* DNA gyrase inhibition than its parent compound **3**, but weaker than the oxalyl derivative **23**. Formation of a hydrogen bond between the acetamide carbonyl group and the protein was also suggested by docking of **45** to *E. coli* GyrB (Figure 7c).

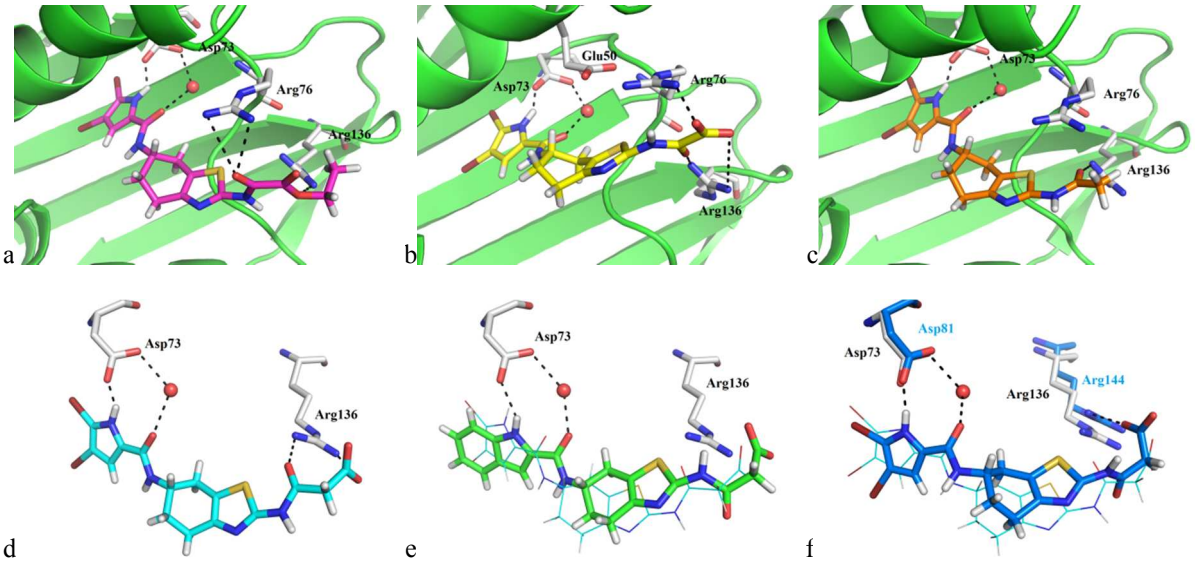

Figure 7. Calculated binding modes of inhibitors a) ester **23** (in *magenta* sticks), b) corresponding carboxylic acid **34** (in *yellow* sticks), c) *N*-acetyl derivative **45** (in *orange* sticks) and d) malonic acid derivative **35** (in *cyan* sticks) in the ATP-binding site of *E. coli* DNA gyrase (PDB entry: 4DUH, in *green* cartoon); e) Overlay of the calculated binding modes of inhibitors **35** (in *cyan* lines) and **40** (in *green* sticks); f) Overlay of calculated binding modes of **35** in the ATP-binding site of *E. coli* (residues in *grey* sticks) and *S. aureus* (PDB entry: 3TTZ, residues in *blue* sticks) DNA gyrase. Figures were prepared by PyMOL.[31]

The calculated binding mode of malonic acid derivative **35** in the *E. coli* GyrB ATP-binding site shows two hydrogen bonds with the guanidine group of Arg136, one with the oxygen of aminocarbonyl group at position 2 of the thiazole moiety and one with the terminal carboxylic acid group (Figure 7d). Because the indole moiety of **40** is bulkier than the 4,5-dibromo-1*H*-pyrrole moiety of **35** (see above), inhibitor **40** is pulled out of the hydrophobic pocket, which could result in weaker hydrogen bonds with Asp73 and the conserved water molecule (Figure 7e). Additionally, the aminocarbonyl group of **40** is rotated by approximately 180° relative to that in **35**. As a consequence, no hydrogen bond is predicted between the aminocarbonyl of **40** and Arg136 and there is possible steric repulsion between the proton of aminocarbonyl of **40** and protons of the guanidine group of Arg136. The terminal carboxylate of **40** is shifted more towards the solvent, as in the case of **35**, which together with the other non-beneficial effects leads to the observed loss of activity of **40**. Similar, although less, rotation of the aminocarbonyl group is also observed in the docking pose of **35** in the *S. aureus* GyrB ATP-binding site, which, together with a shift of inhibitor from a smaller hydrophobic pocket towards the solvent, results in only weak *S. aureus* DNA gyrase inhibition by **35**.

CONCLUSIONS

In summary, structure-based optimization of low micromolar *E. coli* DNA gyrase inhibitors, identified in our in-house library of marine alkaloid oroidin analogs, led to inhibitors with improved inhibitory activity in the nanomolar range. The IC_{50} values of selected compounds, determined in the supercoiling assay, were in good agreement with their IC_{50} values, determined in the ATPase assay, and K_d values, measured in the SPR experiment using the 24 kDa N-terminal part of the GyrB subunit. These results, together with the observed SAR, suggest that these *E. coli* DNA gyrase inhibitors bind to the ATP-binding site of the enzyme. The compounds

were found to be considerably weaker inhibitors of *S. aureus* DNA gyrase and displayed a very weak inhibition of topoisomerase IV from both bacterial strains. Some of the compounds possessed modest antibacterial activity against Gram positive bacterial strains, while being inactive against selected Gram negative bacteria. This extensive structure-activity relationship study, supported by molecular docking calculations, provides good starting points for optimization of 4,5,6-7-tetrahydrobenzo[1,2-*d*]thiazole-based compounds towards more potent, balanced dual inhibitors of DNA gyrase and topoisomerase IV from Gram positive and Gram negative bacteria, with improved antibacterial activity.

EXPERIMENTAL SECTION

Chemistry. All reagents were used as received from commercial sources without further purification unless otherwise indicated. Analytical TLC was performed on Merck silica gel (60 F 254) plates (0.25 mm) and components visualized with staining reagents or ultraviolet light. Flash column chromatography was carried out on silica gel 60 (particle size 240-400 mesh). HPLC analyses were performed on Agilent Technologies 1100 instrument with G1365B UV-VIS detector, G1316A thermostat and G1313A autosampler using Agilent Eclipse Plus C18 column (5 μm, 4.6 × 150 mm) using Method A: Agilent 5μ C18 column; mobile phase: 0.1% trifluoroacetic acid in water (A) and methanol (B); gradient: 90% A to 10% A in 20 min, then 5 min 10 % A; flow rate 1.0 mL/min; injection volume: 10 μL. All tested compounds were ≥95% pure by HPLC. Melting points were determined on a Reichert hot stage microscope and are uncorrected. ^{1}H NMR and ^{13}C NMR spectra were recorded at 400 MHz and 100 MHz, respectively, on a Bruker AVANCE III spectrometer in DMSO-d_6, CD_3OD or $CDCl_3$ solution with TMS as an internal standard at 25 °C. Spectra were assigned using gradient COSY, HSQC

and DEPT experiments. IR spectra were recorded on a Thermo Nicolet Nexus 470 ESP FT-IR spectrometer. Mass spectra were obtained using a VGAnalytical Autospec Q mass spectrometer. Optical rotations were measured on a Perkin-Elmer 241 MC polarimeter. The reported values for specific rotation are the average of 5 successive measurements using an integration time of 5 s. All reported yields are yields of purified products. (*S*)- and (*R*)-4,5,6,7-tetrahydrobenzo[*d*]thiazole-2,6-diamine ((***S*)-18** or (***R*)-18**),[35] and compounds **3-5**[22] were prepared as described. All tested compounds passed the PAINS filter (see below).

General procedure **A**. *Synthesis of compounds **7-9***. A solution of 5,6,7,8-tetrahydroquinazoline-2,6-diamine (**6**) (213 mg, 1.30 mmol) and Na_2CO_3 (138 mg, 1.30 mmol) in DMF (5 mL) was stirred at room temperature for 15 min. Corresponding 2,2,2-trichloro-1-(1*H*-pyrrol-2-yl)ethanone (1.43 mmol) was added and mixture was stirred at 35 °C for 2.5 h. Solvent was removed under reduced pressure, brown residue was suspended in CH_2Cl_2 (20 mL) and filtered. Precipitate was washed with water (70 mL) and dried to yield compound **7**, **8** or **9**.

N-(2-Amino-5,6,7,8-tetrahydroquinazolin-6-il)-4,5-dichloro-1H-pyrrole-2-carboxamide (7). Prepared from **6** (213 mg, 1.30 mmol) and 2,2,2-trichloro-1-(4,5-dichloro-1*H*-pyrrol-2-yl)ethanone (403 mg, 1.43 mmol) according to general procedure **A**. Yield 153 mg (36%); off-white solid; m. p. 309-311 ºC (dec.); IR (ATR): ν 3853, 3735, 3401, 3312, 3202, 3111, 2930, 1598, 1438, 1389, 1336, 922, 770 cm^{-1}; ^{1}H NMR (400 MHz, DMSO-d_6) δ 1.72-1.85 (m, 1H, CH_2), 1.93-2.03 (m, 1H, CH_2), 2.46-2.55 (m, 1H signal overlapped with DMSO-d_5, CH_2), 2.66-2.73 (m, 2H, CH_2), 2.78-2.86 (m, 1H, CH_2), 4.02-4.14 (m, 1H, CH), 6.32 (s, 2H, NH_2), 6.96 (s, 1H, Ar-H), 7.97 (s, 1H, Ar-H), 8.05 (d, 1H, J = 7.0 Hz, NH-C=O), 12.57 (s, 1H, NH) ppm; ^{13}C NMR (100 MHz, DMSO-d_6) δ 27.92, 30.03, 30.44, 44.65, 107.86, 109.89, 114.74, 115.51,

124.83, 158.11, 158.45, 162.07, 164.41 ppm; HRMS m/z for $C_{13}H_{13}Cl_2N_5O$ ($[M+H^+]^+$): calcd 326.0575, found 326.0567; HPLC: t_r 15.06 min (95.8% at 254 nm).

N-(2-Amino-5,6,7,8-tetrahydroquinazolin-6-yl)-4-bromo-1H-pyrrole-2-carboxamide ***(8)***. Prepared from **6** (213 mg, 1.30 mmol) and 1-(4-bromo-1*H*-pyrrol-2-yl)-2,2,2-trichloroethanone (417 mg, 1.43 mmol) according to general procedure **A**. Yield 235 mg (49%); off-white solid; m. p. 275-278 ºC; IR (ATR): ν 3404, 3311, 3198, 3062, 2940, 1633, 1530, 1437, 1330, 922, 770 cm^{-1}; ^1H NMR (400 MHz, DMSO-d_6) δ 1.72-1.85 (m, 1H, CH_2), 1.93-2.03 (m, 1H, CH_2), 2.46-2.55 (m, 1H signal overlapped with DMSO-d_5, CH_2), 2.66-2.73 (m, 2H, CH_2), 2.78-2.85 (m, 1H, CH_2), 4.03-4.14 (m, 1H, CH), 6.31 (s, 2H, NH_2), 6.92 (d, 1H, J = 1.6 Hz, Ar-H), 6.97 (d, 1H, J = 1.6 Hz, Ar-H), 7.97 (s, 1H, Ar-H), 8.03 (d, 1H, J = 7.6 Hz, NH-C=O), 11.86 (s, 1H, NH) ppm; ^{13}C NMR (100 MHz, DMSO-d_6) δ 28.01, 30.10, 30.49, 44.55, 94.84, 111.67, 115.60, 121.14, 126.84, 158.11, 159.05, 162.07, 164.44 ppm; HRMS m/z for $C_{13}H_{14}BrN_5O$ ($[M+H^+]^+$): calcd 336.0451, found 336.0460; HPLC: t_r 12.53 min (95.1% at 254 nm).

N-(2-Amino-5,6,7,8-tetrahydroquinazolin-6-yl)-4,5-dibromo-1H-pyrrole-2-carboxamide ***(9)***. Prepared from **6** (213 mg, 1.30 mmol) and 2,2,2-trichloro-1-(4,5-dichloro-1*H*-pyrrol-2-yl)ethanone (529 mg, 1.43 mmol) according to general procedure **A**. Yield 338 mg (57%); light brown solid; m. p. 309-312 ºC; IR (ATR): ν 3313, 3138, 2933, 1668, 1640, 1556, 1488, 1429, 1337, 1234, 1197, 816 cm^{-1}; ^1H NMR (400 MHz, DMSO-d_6) δ 1.73-1.84 (m, 1H, CH_2), 1.93-2.02 (m, 1H, CH_2), 2.46-2.55 (m, 1H, signal overlapped with DMSO-d_5, CH_2), 2.65-2.73 (m, 2H, CH_2), 2.77-2.86 (m, 1H, CH_2), 4.02-4.13 (m, 1H, CH), 6.31 (s, 2H, NH_2), 6.95 (s, 1H, Ar-H), 7.95-8.00 (m, 2H, NH-C=O, Ar-H), 12.13 (s, 1H, NH) ppm; ^{13}C NMR (100 MHz, DMSO-d_6) δ 27.91, 30.01, 30.45, 44.59, 97.60, 104.63, 112.83, 115.52, 128.22, 158.11, 158.44, 162.08,

164.41 ppm; HRMS m/z for $C_{13}H_{13}Br_2N_5O$ ($[M+H^+]^+$): calcd 412.9554, found 413.9565; HPLC: t_r 15.49 min (99.0% at 254 nm).

*N-(2-Amino-5,6,7,8-tetrahydroquinazolin-6-yl)-1H-indole-2-carboxamide (**10**).* To the solution of indole-2-carboxylic acid (210 mg, 1.30 mmol) in DMF (10 mL) were added Et_3N (362 μL, 2.60 mmol) and TBTU (459 mg, 1.43 mmol). The mixture was stirred at room temperature for 15 min. 5,6,7,8-tetrahydroquinazoline-2,6-diamine (**6**) (213 mg, 1.30 mmol) was then added and the reaction mixture was stirred at room temperature for 2.5 h. Solvent was removed under reduced pressure, brown residue was suspended in CH_2Cl_2 (20 mL) and filtered. Precipitate was washed with $NaHCO_{3(aq)}$ (30 mL), water (30 mL), diethyl ether (15 mL) and dried *in vacuo*. The crude product was recrystallized from ethanol to yield **10** as an off-white solid. Yield 204 mg (51%); m. p. 270-273 ºC; IR (ATR): ν 3397, 3246, 1637, 1541, 1477, 1418, 814, 775, 713 cm^{-1}; ^1H NMR (400 MHz, DMSO-d_6) δ 1.80-1.92 (m, 1H, CH_2), 2.01-2.10 (m, 1H, CH_2), 2.55-2.64 (m, 1H, CH_2), 2.71-2.77 (m, 2H, CH_2), 2.84-2.92 (m, 1H, CH_2), 4.13-4.23 (m, 1H, CH), 6.33 (s, 2H, NH_2), 7.01-7.07 (m, 1H, Ar-H), 7.16-7.21 (m, 2H, 2 × Ar-H), 7.44 (dd, 1H, J_1 = 0.7 Hz, J_2 = 8.2 Hz, Ar-H), 7.61 (d, 1H, J = 8.0 Hz, Ar-H), 8.00 (s, 1H, Ar-H), 8.43 (d, 1H, J = 7.6 Hz, NH-C=O), 11.58 (s, 1H, Ar-NH) ppm; ^{13}C NMR (100 MHz, DMSO-d_6) δ 21.92, 30.12, 30.41, 44.78, 102.77, 112.26, 115.73, 119.66, 121.44, 123.24, 127.01, 131.68, 136.37, 157.89, 160.60, 161.61, 164.68 ppm; HRMS m/z for $C_{17}H_{17}N_5O$ ($[M+H^+]^+$): calcd 308.1509, found 308.1511; HPLC: t_r 13.88 min (99.2% at 254 nm).

General procedure **B**. *Synthesis of compounds **11** and **12**.* To the suspension of compound **9** or **10** (1.50 mmol) in DMF (7 mL) was added Et_3N (230 μL, 1.65 mmol), with a following dropwise addition of methyl 3-chloro-3-oxopropanoate (242 μL, 2.25 mmol). The reaction mixture was then stirred overnight at room temperature, $NaHCO_{3(aq)}$ (0.5 mL) was added and the

solvent was removed under reduced pressure. The brown residue was suspended in THF (50 mL), filtered and the filtrate was concentrated *in vacuo*. The crude product was then purified by column chromatography with dichloromethane/methanol as an eluent to afford compound **11** or **12**.

*Methyl 3-((6-(4,5-dibromo-1H-pyrrole-2-carboxamido)-5,6,7,8-tetrahydroquinazolin-2-yl)amino)-3-oxopropanoate (**11**).* Prepared from **9** (623 mg, 1.50 mmol) according to general procedure **B**. Yield 363 mg (47%); off-white solid; m. p. 187-189 ºC; IR (ATR): ν 3366, 3161, 2951, 1718, 1635, 1509, 1332, 1221, 971, 821 cm^{-1}; ^1H NMR (400 MHz, DMSO-d_6) δ 1.81-1.93 (m, 1H, CH_2), 1.99-2.08 (m, 1H, CH_2), 2.66 (dd, 1H, J_1 = 9.2 Hz, J_2 = 16.2 Hz, CH_2), 2.81-2.89 (m, 2H, CH_2), 3.00 (dd, 1H, J_1 = 5.0 Hz, J_2 = 16.6 Hz, CH_2), 3.63 (s, 3H, CH_3), 3.68 (s, 2H, CH_2-C=O), 4.12-4.23 (m, 1H, CH), 7.01 (s, 1H, Ar-H), 8.10 (d, 1H, J = 7.4 Hz, NH-C=O), 8.37 (s, 1H, Ar-H), 10.67 (s, 1H, Ar-NH-C=O), 12.71 (s, 1H, NH) ppm; ^{13}C NMR (100 MHz, DMSO-d_6) δ 27.39, 29.76, 30.43, 43.94, 44.04, 51.83, 97.75, 104.56, 112.92, 122.95, 128.02 (2C), 155.33, 158.14, 158.42, 165.45, 168.12 ppm; HRMS m/z for $C_{17}H_{17}Br_2N_5O_4$ ($[M+H^+]^+$): calcd 513.9726, found 513.9739; HPLC: t_r 18.03 min (96.2% at 254 nm).

*Methyl 3-((6-(1H-indole-2-carboxamido)-5,6,7,8-tetrahydroquinazolin-2-yl)amino)-3-oxopropanoate (**12**).* Prepared from **10** (461 mg, 1.50 mmol) according to general procedure **B**. Yield 306 mg (50%); white solid; m. p. 190-192 ºC; IR (ATR): ν 3267, 3133, 2934, 1736, 1682, 1634, 1542, 1506, 1416, 1342, 1206, 1158, 816 cm^{-1}; ^1H NMR (400 MHz, DMSO-d_6) δ 1.89-2.00 (m, 1H, CH_2), 2.06-2.15 (m, 1H, CH_2), 2.75 (dd, 1H, J_1 = 9.4 Hz, J_2 = 16.5 Hz, CH_2), 2.86-2.93 (m, 2H, CH_2), 3.06 (dd, 1H, J_1 = 4.8 Hz, J_2 = 16.1 Hz, CH_2), 3.64 (s, 3H, CH_3), 3.69 (s, 2H, CH_2-C=O), 4.22-4.33 (m, 1H, CH), 7.01-7.07 (m, 1H, Ar-H), 7.16-7.21 (m, 2H, 2 × Ar-H), 7.44 (dd, 1H, J_1 = 0.8 Hz, J_2 = 8.3 Hz, Ar-H), 7.62 (d, 1H, J = 7.7 Hz, Ar-H), 8.40 (s, 1H, Ar-H), 8.48

(d, 1H, J = 7.6 Hz, NH-C=O), 10.68 (s, 1H, Ar-NH-C=O), 11.59 (d, 1H, J = 1.6 Hz, NH) ppm; ^{13}C NMR (100 MHz, DMSO-d_6) δ 27.51, 29.96, 30.47, 44.06, 44.18, 51.84, 54.90, 102.83, 112.26, 119.67, 121.45, 123.06, 123.27, 126.99, 131.60, 136.38, 155.35, 158.16, 160.68, 165.49, 168.13 ppm; HRMS m/z for $C_{21}H_{21}N_5O_4$ ($[M+H^+]^+$): calcd 408.1672, found 408.1660; HPLC: t_r 16.64 min (98.9% at 254 nm).

General procedure **C**. *Synthesis of compounds **13** and **14**.* To the solution of 3-(benzyloxy)-3-oxopropanoic acid (97 mg, 0.50 mmol) in DMF (5 mL) were added Et_3N (139 μL, 1.00 mmol) and TBTU (177 mg, 0.55 mmol). The mixture was stirred at room temperature for 15 min. Compound **9** or **10** (0.50 mmol) was then added and the reaction mixture was stirred at 40 ºC for 4 h. Solvent was removed *in vacuo* and the brown residue was suspended in ethyl acetate (25 mL). The suspension was washed with water (25 mL), $NaHCO_{3(aq)}$ (25 mL), 10% citric acid (25 mL) and brine (20 mL). Organic phase was dried over Na_2SO_4 and concentrated under reduced pressure. The crude product was then purified by column chromatography with ethyl acetate as an eluent to afford compound **13** or **14**.

*Benzyl 3-((6-(4,5-dibromo-1H-pyrrole-2-carboxamido)-5,6,7,8-tetrahydroquinazolin-2-yl)amino)-3-oxopropanoate (**13**).* Prepared from **9** (208 mg, 0.50 mmol) according to general procedure **C**. Yield 74 mg (25%); off-white solid; m. p. 233-235 ºC; IR (ATR): ν 3267, 3132, 2933, 1639, 1555, 1501, 1415, 1337, 1197, 1155, 972, 815 cm^{-1}; ^{1}H NMR (400 MHz, DMSO-d_6) δ 1.78-1.90 (m, 1H, CH_2), 1.96-2.06 (m, 1H, CH_2), 2.63 (dd, 1H, J_1 = 9.1 Hz, J_2 = 16.4 Hz, CH_2), 2.76-2.83 (m, 2H, CH_2), 2.97 (dd, 1H, J_1 = 5.3 Hz, J_2 = 16.4 Hz, CH_2), 3.77 (s, 2H, CH_2-C=O), 4.10-4.20 (m, 1H, CH), 5.13 (s, 2H, O-CH_2), 7.01 (s, 1H, Ar-H), 7.31-7.39 (m, 5H, 5 × Ar-H), 8.09 (d, 1H, J = 7.3 Hz, NH-C=O), 8.28 (s, 1H, Ar-H), 10.67 (s, 1H, Ar-NH-C=O), 12.72 (s, 1H, NH) ppm; ^{13}C NMR (100 MHz, DMSO-d_6) δ 27.39, 29,74, 30.43, 43.93, 44.36, 65.89,

97.74, 104.62, 112.91, 122.83, 128.01 (3C: 2 signals overlapped), 128.09, 128.28, 128.34 (2C), 135.85, 155.31, 158.06, 158.43, 165.42, 167.46 ppm; HRMS m/z for $C_{23}H_{21}Br_2N_5O_4$ ($[M+H^+]^+$): calcd 590.0039, found 590.0050; HPLC: t_r 19.78 min (90.9% at 254 nm).

*Benzyl 3-((6-(1H-indole-2-carboxamido)-5,6,7,8-tetrahydroquinazolin-2-yl)amino)-3-oxopropanoate (**14**).* Prepared from **10** (154 mg, 0.50 mmol) according to general procedure **C**. Yield 68 mg (28%); yellow solid; m. p. 206-209 ºC; IR (ATR): ν 3267, 3134, 2933, 1719, 1638, 1550, 1506, 1416, 1314, 1199, 1155, 967, 811 cm^{-1}; ^1H NMR (400 MHz, DMSO-d_6) δ 1.86-1.97 (m, 1H, CH_2), 2.03-2.11 (m, 1H, CH_2), 2.73 (dd, 1H, J_1 = 9.8 Hz, J_2 =16.5 Hz, CH_2), 2.80-2.87 (m, 2H, CH_2), 3.03 (dd, 1H, J_1 = 5.0 Hz, J_2 = 16.1 Hz, CH_2), 3.78 (s, 2H, CH_2-C=O), 4.21-4.31 (m, 1H, CH), 5.14 (s, 2H, O-CH_2), 7.02-7.07 (m, 1H, Ar-H), 7.16-7.21 (m, 2H, 2 × Ar-H), 7.31-7.40 (m, 5H, 5 × Ar-H), 7.44 (dd, 1H, J_1 = 0.9 Hz, J_2 =8.3 Hz, Ar-H), 7.62 (dd, 1H, J_1 = 0.6 Hz, J_2 = 7.9 Hz, Ar-H), 8.31 (s, 1H, Ar-H), 8.48 (d, 1H, J = 7.5 Hz, NH-C=O), 10.68 (s, 1H, Ar-NH-C=O), 11.60 (d, 1H, J = 1.5 Hz, NH) ppm; ^{13}C NMR (100 MHz, DMSO-d_6) δ 27.50, 29.93, 30.46, 44.17, 44.36, 65.89, 102.82, 112.26, 119.87, 121.45, 122.95, 123.28, 127.00, 128.02 (3C: 2 signals overlapped), 128.35 (2C), 128.41, 131.61, 135.86, 136.39, 155.33, 158.07, 160.68, 165.47, 167.47 ppm; HRMS m/z for $C_{27}H_{25}N_5O_4$ ($[M+H^+]^+$): calcd 484.1985, found 484.1987; HPLC: t_r 18.45 min (98.5% at 254 nm).

*N-(2-Acetamido-5,6,7,8-tetrahydroquinazolin-6-yl)-1H-indole-2-carboxamide (**17**).* To the solution of benzyl 3-((6-(1*H*-indole-2-carboxamido)-5,6,7,8-tetrahydroquinazolin-2-yl)amino)-3-oxopropanoate (**16**) (60 mg, 0.124 mmol) in a mixture of methanol (3 mL) and THF (3 mL) was added 10% Pd/C (10 mg) and the reaction mixture was stirred under hydrogen atmosphere for 3 h. The catalyst was filtered off and the solvent was removed under reduced pressure. The crude product was then triturated with diethyl ether (2 × 15 mL) to afford compound **17** as a white

solid. Yield: 36 mg (85%); m. p. 257-260 ºC; IR (ATR): ν 3272, 3145, 2933, 1634, 1552, 1505, 1415, 1372, 1311, 1233, 806 cm^{-1}; ^1H NMR (400 MHz, DMSO-d_6) δ 1.89-2.01 (m, 1H, CH_2), 2.06-2.15 (m, 1H, CH_2), 2.17 (s, 3H, CH_3), 2.75 (dd, 1H, J_1 = 9.5 Hz, J_2 = 16.2 Hz, CH_2), 2.88-2.94 (m, 2H, CH_2), 3.06 (dd, 1H, J_1 = 4.8 Hz, J_2 = 16.1 Hz, CH_2), 4.23-4.33 (m, 1H, CH), 7.01-7.07 (m, 1H, Ar-H), 7.16-7.21 (m, 2H, 2 x Ar-H), 7.44 (dd, 1H, J_1 = 0.9 Hz, J_2 = 8.2 Hz, Ar-H), 7.62 (dd, 1H, J_1 = 0.7 Hz, J_2 = 7.9 Hz, Ar-H), 8.39 (s, 1H, Ar-H), 8.48 (d, 1H, J = 7.5 Hz, NH-C=O), 10.40 (s, 1H, Ar-NH-C=O), 11.59 (d, 1H, J = 1.7 Hz, NH) ppm; ^{13}C NMR (100 MHz, DMSO-d_6) δ 24.45, 27.58, 30.05, 30.50, 44.25, 102.83, 112.26, 119.67, 121.45, 122.82, 123.27, 127.00, 131.61, 136.39, 155.74, 158.09, 160.68, 165.40, 168.83 ppm; HRMS m/z for $C_{19}H_{19}N_5O_2$ ($[M+H^+]^+$): calcd 350.1617, found 350.1614; HPLC: t_r 15.23 min (93.0% at 254 nm).

General procedure **D.** *Synthesis of compounds* **19** and **22**. A solution of (*S*)- or (*R*)-4,5,6,7-tetrahydrobenzo[1,2-*d*]thiazole-2,6-diamine (1 mmol) and Na_2CO_3 (1 mmol) in *N,N*-dimethylformamide (5 mL) was stirred at room temperature for 15 min. Then 2,2,2-trichloro-1-(4,5-dichloro-1*H*-pyrrol-2-yl)ethan-1-one or 2,2,2-trichloro-1-(4,5-dibromo-1*H*-pyrrol-2-yl)ethan-1-one (1.1 mmol) was added and the mixture stirred at 40 °C for 2.5 h. Solvent was removed under reduced pressure and purified by column chromatography using dichloromethane/methanol (20:1) as eluent.

*(R)-N-(2-Amino-4,5,6,7-tetrahydrobenzo[1,2-d]thiazol-6-yl)-4,5-dibromo-1H-pyrrole-2-carboxamide (**19**).* Prepared from (*R*)-4,5,6,7-tetrahydrobenzo[1,2-*d*]thiazole-2,6-diamine (0.098 g, 0.58 mmol) and 2,2,2-trichloro-1-(4,5-dibromo-1*H*-pyrrol-2-yl)ethan-1-one (0.214 g, 0.58 mmol) according to general procedure **D**. Yield: 145.0 mg (59.7%); yellowish crystals; m.p. 123-125 °C; $[\alpha]_D$ +27.4 (*c* 0.23, MeOH); IR (ATR) ν 3113, 2928, 1710, 1619, 1557, 1513, 1414,

1390, 1370, 1312, 1228 cm^{-1}; ^1H NMR (400 MHz, DMSO-d_6): δ 1.72-1.82 (m, 1H, H_A-7), 1.90-1.93 (m, 1H, H_B-7), 2.44-2.53 (m, 3H, signal partially overlapped with DMSO-d_5, H-5, H_A-4), 2.78 (dd, 1H, J_1 = 4.8 Hz, J_2 = 15.0 Hz, H_B-4), 4.08-4.18 (m, 1H, CHNH), 6.68 (s, 2H, NH_2), 6.99 (s, 1H, Ar-H), 8.05 (d, 1H, J = 7.6 Hz, CONH), 12.68 (s, 1H, Ar-NH) ppm; ^{13}C NMR (100 MHz, DMSO-d_6): δ 24.8, 28.5, 28.6, 45.4, 97.6, 104.3, 112.1, 112.7, 127.9, 144.1, 158.2, 166.0 ppm; HRMS (ESI^+) m/z for $C_{12}H_{13}Br_2N_4OS$ ($[M+H]^+$): calcd 418.9177, found 418.9172; HPLC: t_r 18.07 min (100.0%, at 254 nm).

*(S)-N-(2-Amino-4,5,6,7-tetrahydrobenzo[1,2-d]thiazol-6-yl)-4,5-dichloro-1H-pyrrole-2-carboxamide (**22**).* Prepared from (*S*)-4,5,6,7-tetrahydrobenzo[1,2-*d*]thiazole-2,6-diamine (0.180 g, 1.07 mmol) and 2,2,2-trichloro-1-(4,5-dichloro-1*H*-pyrrol-2-yl)ethan-1-one (0.300 g, 1.07 mmol) according to general procedure **D**. Yield: 190.0 mg (53.8%); yellowish crystals; m.p. 250 °C (decomposition); $[\alpha]_D$ -31.8 (*c* 0.24, MeOH); IR (ATR) ν 3117, 2910, 1612, 1562, 1512, 1429, 1397, 1366, 1312, 1271, 1230, 1170, 1095, 1017 cm^{-1}; ^1H NMR (400 MHz, DMSO-d_6): δ 1.71-1.83 (m, 1H, H_A-7), 1.90-1.94 (m, 1H, H_B-7), 2.43-2.54 (m, 3H, signal partially overlapped with DMSO-d_5, H-5, H_A-4), 2.78 (dd, 1H, J_1 = 5.1 Hz, J_2 =15.3 Hz, H_B-4), 4.09-4.18 (m, 1H, CHNH), 6.68 (s, 2H, NH_2), 6.96 (s, 1H, Ar-H), 8.07 (d, 1H, J = 7.7 Hz, CONH), 12.72 (s, 1H, Ar-NH) ppm; ^{13}C NMR (100 MHz, DMSO-d_6): δ 24.9, 28.6, 28.7, 45.5, 107.9, 109.9, 112.2, 114.7, 124.8, 144.0, 158.4, 166.2 ppm; HRMS (ESI^+) m/z for $C_{12}H_{13}Cl_2N_4OS$ ($[M+H]^+$): calcd 331.0187; found 331.0183; HPLC: t_r 15.32 min (100.0% at 254 nm).

General procedure **E.** *Synthesis of compounds* **20** and **21.** To a solution of 5-fluoro-1*H*-indole-2-carboxylic acid or 5-chloro-1*H*-indole-2-carboxylic acid (1 mmol) in dichloromethane (10 mL) were added Et_3N (2 mmol) and TBTU (1.1 mmol) and the mixture stirred at room temperature for 15 min. Then (*S*)-4,5,6,7-tetrahydrobenzo[1,2-*d*]thiazole-2,6-diamine (1 mmol) and Et_3N

(2 mmol) were added and the reaction mixture was stirred at room temperature for 2.5 h. The reaction mixture was diluted with dichloromethane (15 mL) and washed with saturated aqueous $NaHCO_3$ solution (2 × 15 mL). Combined water phases were extracted with dichloromethane (20 mL). Combined organic phases were dried over Na_2SO_4, filtered and the solvent removed under reduced pressure.

*(S)-N-(2-Amino-4,5,6,7-tetrahydrobenzo[1,2-d]thiazol-6-yl)-5-fluoro-1H-indole-2-carboxamide (**20**)*. Prepared from 5-fluoro-1*H*-indole-2-carboxylic (0.150 g, 0.88 mmol) and (*S*)-4,5,6,7-tetrahydrobenzo[1,2-*d*]thiazole-2,6-diamine (0.141 g, 0.88 mmol) according to general procedure **E**. The crude product was purified by flash column chromatography using dichloromethane/methanol (40:1) as eluent. Yield: 80.0 mg (28.9%); yellow solid; m.p. 279-282 °C; $[\alpha]_D$ -38.9 (*c* 0.22, MeOH); IR (ATR) ν 3633, 3276, 2948, 2843, 1627, 1584, 1537, 1508,1488, 1445, 1423, 1372, 1320, 1300, 1279, 1262, 1223, 1158, 1111, 1074, 1019, 974, 954, 915, 880, 863, 798, 768, 757, 735, 674, 629, 615, 602, 588 cm^{-1}; ^1H NMR (400 MHz, DMSO-d_6): δ 1.80-1.89 (m, 1H, H_A-7), 1.94-2.02 (m, 1H, H_B-7), 2.52-2.60 (m, 3H, H-5, H_A-4), 2.84 (dd, 1H, J_1 = 5.8 Hz, J_2 =14.8 Hz, H_B-4), 4.17-4.26 (m, 1H, C<u>H</u>NH), 6.70 (s, 2H, NH_2), 6.99-7.06 (m, 1H, Ar-H), 7.17-7.20 (m, 1H, Ar-H), 7.43-7.46 (m, 1H, Ar-H), 7.70 (d, 1H, J = 2.1 Hz, Ar-H), 8.59 (d, 1H, J = 7.8 Hz, CONH), 11.87 (s, 1H, Ar-NH) ppm; ^{13}C NMR (100 MHz, DMSO-d_6): δ 25.1, 28.7, 28.8, 45.8, 102.8 (d, $^3J_{CF}$ = 5.0 Hz), 105.6 (d, $^2J_{CF}$ = 23.0 Hz), 111.9 (d, $^2J_{CF}$ = 26.0 Hz), 112.3, 113.4 (d, $^3J_{CF}$ = 9.7 Hz), 127.1 (d, $^3J_{CF}$ = 10.6 Hz), 133.2 (d, $^2J_{CF}$ = 32.3 Hz), 144.1, 155.9, 158.2 (d, $^1J_{CF}$ = 232 Hz), 160.2, 166.2 ppm; HRMS (ESI^+) m/z for $C_{16}H_{16}FN_4OS$ ($[M+H]^+$): calcd 331.1029, found 331.1031; HPLC: t_r 14.885 min (100.0% at 254 nm, 100% at 210 nm).

*(S)-N-(2-Amino-4,5,6,7-tetrahydrobenzo[1,2-d]thiazol-6-yl)-5-chloro-1H-indole-2-carboxamide (**21**).* Prepared from 5-chloro-1*H*-indole-2-carboxylic (0.150 g, 0.77 mmol) and (*S*)-4,5,6,7-tetrahydrobenzo[1,2-*d*]thiazole-2,6-diamine (0.130 g, 0.77 mmol) according to general procedure **E**. The crude product was purified by flash column chromatography using dichloromethane/methanol (40:1) as eluent. Yield: 88.0 mg (33.0%); yellow solid; m.p. 265-267 °C; $[\alpha]_D$ +31.4 (*c* 0.18, MeOH); IR (ATR) ν 3635, 3275, 3098, 2365, 1696, 1625, 1581, 1536, 1458, 1383, 1323, 1285, 1240, 1217, 1194, 1165, 1124, 1098, 1060, 1003, 916, 876, 812, 797, 768, 737, 714, 670, 631, 599, 587, 573 cm^{-1}; ^1H NMR (400 MHz, DMSO-d_6): δ 1.79-1.89 (m, 1H, H_A-7), 1.95-2.01 (m, 1H, H_B-7), 2.52-2.59 (m, 3H, H-5, H_A-4), 2.84 (dd, 1H, J_1 = 5.5 Hz, J_2 =14.8 Hz, H_B-4), 4.17-4.26 (m, 1H, C<u>H</u>NH), 6.70 (s, 2H, NH_2), 7.04 (dt, 1H, J_1 = 2.6 Hz, J_1 = 9.4 Hz, Ar-H), 7.18 (d, 1H, J_1 = 1.2 Hz, Ar-H), 7.41 (dt, 2H, J_1 = 3.6 Hz, J_1 = 9.4 Hz, Ar-H), 8.50 (d, 1H, J = 7.8 Hz, CONH), 11.71 (s, 1H, Ar-NH) ppm; ^{13}C NMR (100 MHz, DMSO-d_6): δ 25.1, 28.7, 28.8, 45.8, 102.3, 112.3, 113.8, 120.5, 123.3, 124.4, 128.1, 133.2, 134.8, 144.3, 160.2, 166.2 ppm; HRMS (ESI^+) m/z for $C_{16}H_{16}ClN_4OS$ ($[M+H]^+$): calcd 347.0733, found 347.0728; HPLC: t_r 16.643 min (95.5% at 254 nm).

General procedure **F.** *Synthesis of compounds* **23-33**. To a solution of amine (1 mmol) and Et_3N (1.1 mmol) in 1,4-dioxane (5 mL), ethyl 2-chloro-2-oxoacetate, methyl 3-chloro-3-oxopropanoate, methyl 4-chloro-4-oxobutanoate or acetyl chloride (1.5 mmol) was added drop wise. Reaction mixture was stirred at room temperature for 4-12 h. Saturated aqueous $NaHCO_3$ solution was added (5 mL) and the product extracted with ethyl acetate (3 × 10 mL). Combined organic phases were washed with brine (20 mL), dried over Na_2SO_4, filtered and the solvent removed under reduced pressure. Crude product was purified by flash column chromatography using *n*-hexane/ethyl acetate (4:1) as eluent.

*Ethyl (S)-2-((6-(4,5-dibromo-1H-pyrrole-2-carboxamido)-4,5,6,7-tetrahydrobenzo[1,2-d]thiazol-2-yl)amino)-2-oxoacetate (**23**).* Prepared from **3** (0.400 g, 0.95 mmol) and ethyl 2-chloro-2-oxoacetate (0.160 mL, 1.43 mmol) according to general procedure **F**. Yield: 250.0 mg (50.5%); yellow crystals; m.p. 154-156 °C; $[\alpha]_D$ +4.2 (*c* 0.20, MeOH); IR (ATR) ν 3120, 2931, 1738, 1696, 1630, 1557, 1511, 1414, 1392, 1369, 1257, 1229, 1179, 1155, 1093, 1014 cm^{-1}; ^1H NMR (400 MHz, DMSO-d_6): δ 1.30 (t, 3H, J = 7.1 Hz, $CH_2C\underline{H}_3$), 1.81-1.93 (m, 1H, H_A-7), 1.99-2.03 (m, 1H, H_B-7), 2.66 (dd, 1H, J_1 = 8.6 Hz, J_2 =16.6 Hz, H_A-5), 2.72-2.81 (m, 2H, H_B-5, H_A-4), 3.03 (dd, 1H, J_1 = 4.9 Hz, J_2 =16.0 Hz, H_B-4), 4.19-4.23 (m, 1H, C<u>H</u>NH), 4.29 (q, 2H, J = 7.1 Hz, $C\underline{H}_2CH_3$), 7.01 (d, 1H, J = 2.5 Hz, Ar-H), 8.13 (d, 1H, J = 7.6 Hz, CON<u>H</u>CH), 12.71 (d, 1H, J = 2.1 Hz, NH), 12.88 (br s, 1H, NH) ppm; ^{13}C NMR (100 MHz, DMSO-d_6): δ 13.7, 24.6, 28.3, 28.4, 45.0, 62.4, 97.8, 104.6, 112.9, 120.7, 128.0, 144.1, 158.4 ppm; HRMS (ESI^+) m/z for $C_{16}H_{17}Br_2N_4O_4S$ ($[M+H]^+$): calcd 518.9337, found 518.9336. HPLC: t_r 20.53 min (95.8% at 254 nm).

*Methyl (S)-3-((6-(4,5-dibromo-1H-pyrrole-2-carboxamido)-4,5,6,7-tetrahydrobenzo[1,2-d]thiazol-2-yl)amino)-3-oxopropanoate (**24**).* Prepared from **3** (0.400 g, 0.95 mmol) and methyl 3-chloro-3-oxopropanoate (0.153 mL, 1.43 mmol) according to general procedure **F**. Yield: 398.0 mg (80.4%); off-white crystals; m.p. 141-143 °C; $[\alpha]_D$ -2.8 (*c* 0.20, MeOH); IR (ATR) ν 3172, 2950, 1737, 1626, 1556, 1515, 1433, 1413, 1391, 1329, 1212, 1153, 1016 cm^{-1}; ^1H NMR (400 MHz, DMSO-d_6): δ 1.81-1.91 (m, 1H, H_A-7), 1.95-2.02 (m, 1H, H_B-7), 2.59-2.73 (m, 3H, H-5, H_A-4), 2.99 (dd, 1H, J_1 = 5.4 Hz, J_2 =15.8 Hz, H_B-4), 3.57 (s, 2H, $COCH_2CO$), 3.65 (s, 3H, $COOCH_3$), 4.13-4.24 (m, 1H, C<u>H</u>NH), 6.99-7.01 (m, 1H, Ar-H), 8.09 (d, 1H, J = 7.6 Hz, CON<u>H</u>CH), 12.14 (s, 1H, NH), 12.70 (d, 1H, J = 2.3 Hz, NH) ppm; ^{13}C NMR (100 MHz, DMSO-d_6): δ 24.6, 28.3, 28.5, 41.9, 45.0, 52.1, 97.7, 104.5, 112.9, 119.6, 128.0, 143.6, 155.3,

158.3, 163.8, 167.5 ppm; HRMS (ESI^+) m/z for $C_{16}H_{17}Br_2N_4O_4S$ ($[M+H]^+$): calcd 518.9337, found 518.9342; HPLC: t_r 18.90 min (100% at 254 nm).

*Methyl (S)-4-((6-(4,5-dibromo-1H-pyrrole-2-carboxamido)-4,5,6,7-tetrahydrobenzo[1,2-d]thiazol-2-yl)amino)-4-oxobutanoate (**25**).* Prepared from **3** (0.400 g, 0.95 mmol) and methyl 4-chloro-4-oxobutanoate (0.175 mL, 1.43 mmol) according to general procedure **F**. Yield: 434.0 mg (85.3%); yellow crystals; m.p. 93-95 °C; $[\alpha]_D$ +22.1 (*c* 0.21, MeOH); IR (ATR) ν 3125, 2936, 1739, 1696, 1630, 1562, 1519, 1433, 1396, 1369, 1330, 1257, 1230, 1178, 1155, 1115, 1014 cm^{-1}; ^1H NMR (400 MHz, CD_3OD): δ 1.88-1.98 (m, 1H, H_A-7), 2.07-2.16 (m, 1H, H_B-7), 2.61-2.79 (m, 7H, H-5, H_A-4, $COCH_2CH_2CO$), 3.06 (dd, 1H, J_1 = 5.1 Hz, J_2 =15.3 Hz, H_B-4), 3.68 (s, 3H, $COOCH_3$), 4.25-4.32 (m, 1H, CHNH), 6.88 (s, 1H, Ar-H), 8.09 (d, 1H, *J* = 8.0 Hz, CONHCH) ppm, signals for pyrrole-NH and $NHCOCH_2CH_2$ cannot be seen in the spectrum; ^{13}C NMR (100 MHz, CD_3OD): δ 24.5, 28.2, 28.3, 28.4, 29.7, 46.0, 50.9, 98.5, 104.7, 113.2, 120.0, 127.4, 145.6, 154.5, 159.9, 170.5, 173.2 ppm; HRMS (ESI^+) m/z for $C_{16}H_{17}Cl_2N_4O_4S$ ($[M+H]^+$): calcd: 431.0348, found 431.0336. HPLC: t_r 20.46 min (95.4% at 254 nm).

*Methyl (R)-3-((6-(4,5-dibromo-1H-pyrrole-2-carboxamido)-4,5,6,7-tetrahydrobenzo[1,2-d]thiazol-2-yl)amino)-3-oxopropanoate (**26**).* Prepared from **19** (0.081 g, 0.19 mmol) and methyl 3-chloro-3-oxopropanoate (0.031 mL, 0.29 mmol) according to general procedure **F**. Yield: 79.0 mg (78.8%); off-white crystals; m.p. 135-138 °C; $[\alpha]_D$ +10.5 (*c* 0.20, MeOH); IR (ATR) ν 3173, 2950, 1738, 1682, 1627, 1556, 1515, 1434, 1414, 1392, 1327, 1289, 1215, 1151, 1077, 1012 cm^{-1}; ^1H NMR (400 MHz, DMSO-d_6): δ 1.81-1.91 (m, 1H, H_A-7), 1.95-2.02 (m, 1H, H_B-7), 2.59-2.73 (m, 3H, H-5, H_A-4), 2.99 (dd, 1H, J_1 = 5.4 Hz, J_2 =15.8 Hz, H_B-4), 3.57 (s, 2H, $COCH_2CO$), 3.65 (s, 3H, $COOCH_3$), 4.13-4.24 (m, 1H, CHNH), 7.01 (s, 1H, Ar-H), 8.09 (d, 1H, *J* = 7.6 Hz, CONHCH), 12.14 (s, 1H, NH), 12.70 (d, 1H, *J* = 2.3 Hz, NH) ppm; ^{13}C NMR (100 MHz,

DMSO-d_6): δ 24.6, 28.3, 28.5, 41.9, 45.0, 52.1, 97.7, 104.5, 112.9, 119.6, 128.0, 143.6, 155.3, 158.3, 163.8, 167.5 ppm; HRMS (ESI$^-$) m/z for $C_{16}H_{15}Br_2N_4O_4S$ ([M-H]$^-$): calcd 516.9181, found 516.9172; HPLC: t_r 19.079 min (97.1% at 254 nm, 99.9% at 280 nm).

*Methyl (S)-3-((6-(4-bromo-1H-pyrrole-2-carboxamido)-4,5,6,7-tetrahydrobenzo[1,2-d]thiazol-2-yl)amino)-3-oxopropanoate (**27**).* Prepared from **4** (0.098 g, 0.29 mmol) and methyl 3-chloro-3-oxopropanoate (0.046 mL, 0.43 mmol) according to general procedure **F**. Yield: 109 mg (86.0%); brown crystals; m.p. 145-147 °C; $[\alpha]_D$ +1.2 (*c* 0.23, MeOH); IR (ATR) ν 3184, 3063, 2951, 1737, 1683, 1625, 1557, 1516, 1435, 1387, 1332, 1256, 1208, 1137, 1015 cm^{-1}; ^{1}H NMR (400 MHz, DMSO-d_6): δ 1.80-2.10 (m, 2H, H-7), 2.53-2.82 (m, 3H, H-5, H_A-4), 2.94-3.08 (m, 1H, H_B-4), 3.60 (s, 2H, $COCH_2CO$), 3.68 (s, 3H, $COOCH_3$), 4.15-4.28 (m, 1H, C<u>H</u>NH), 6.94 (s, 1H, Ar-H), 7.00 (s, 1H, Ar-H), 8.10 (s, 1H, CON<u>H</u>CH), 11.87 (s, 1H, NH), 12.15 (s, 1H, NH) ppm; ^{13}C NMR (100 MHz, DMSO-d_6): δ 24.6, 28.4, 28.6, 41.9, 45.1, 52.1, 94.8, 111.7, 119.7, 121.2, 126.7, 143.5, 155.1, 159.0, 163.8, 167.5 ppm; HRMS (ESI$^-$) m/z for $C_{16}H_{17}BrN_4O_4S$ ([M-H]$^-$): calcd 439.0076, found 439.0075; HPLC: t_r 17.055 min (99.1% at 254 nm, 98.8% at 280 nm).

*Ethyl (S)-2-((6-(1H-indole-2-carboxamido)-4,5,6,7-tetrahydrobenzo[1,2-d]thiazol-2-yl)amino)-2-oxoacetate (**28**).* Prepared from **5** (0.250 g, 0.80 mmol) and ethyl 2-chloro-2-oxoacetate (0.137 mL, 1.20 mmol) according to general procedure **F**. Yield: 257 mg (77.9%); yellow crystals; m.p. 132-135 °C; $[\alpha]_D$ +20.0 (*c* 0.21, MeOH); IR (ATR) ν 3179, 2934, 1686, 1625, 1529, 1437, 1366, 1265, 1221, 1158, 1116, 1082, 1017, 872, 845, 812, 768, 747, 675, 659, 639, 605, 590, 584, 574, 558 cm^{-1}; ^{1}H NMR (400 MHz, DMSO-d_6): δ 1.31 (t, 3H, J = 7.1 Hz, $CH_2C\underline{H_3}$), 1.90-2.00 (m, 1H, H_A-7), 2.05-2.11 (m, 1H, H_B-7), 2.71-2.81 (m, 3H, H-5, H_A-4), 3.08 (dd, 1H, J_1 = 5.4 Hz, J_2 = 15.5 Hz, H_B-4), 4.24-4.6 (m, 3H, C<u>H</u>NH, $C\underline{H_2}CH_3$), 7.04 (ddd, 1H, J_1

= 1.0 Hz, J_2 = 7.0 Hz, J_3 = 8.0 Hz, Ar-H), 7.16-7.21 (m, 2H, Ar-H), 7.44 (dd, 1H, J_1 = 0.9 Hz, J_2 = 8.2 Hz, Ar-H), 7.62 (dd, 1H, J_1 = 0.7 Hz, J_2 = 7.9 Hz, Ar-H), 8.50 (d, 1H, J = 7.8 Hz, CONHCH), 11.59 (d, 1H, J = 1.6 Hz, NH), 12.92 (s, 1H, NH) ppm; ^{13}C NMR (100 MHz, DMSO-d_6): δ 13.8, 24.3, 28.3, 28.4, 45.3, 62.3, 102.8, 112.3, 119.7, 121.5, 123.3, 127.0, 131.6, 136.4, 160.6 ppm; HRMS (ESI$^+$) m/z for $C_{20}H_{21}N_4O_4S$ ($[M+H]^+$): calcd 413.1284, found 413.1280; HPLC: t_r 18.911 min (95.2% at 254 nm).

*Methyl (S)-3-((6-(1H-indole-2-carboxamido)-4,5,6,7-tetrahydrobenzo[1,2-d]thiazol-2-yl)amino)-3-oxopropanoate (**29**).* Prepared from **5** (0.250 g, 0.80 mmol) and methyl 3-chloro-3-oxopropanoate (0.129 mL, 1.20 mmol) according to general procedure **F**. Yield: 130 mg (39.4%); yellow crystals; m.p. 122-124 °C; $[\alpha]_D$ +11.3 (*c* 0.18, MeOH); IR (ATR) ν 3745, 3274, 2949, 2360, 2042, 2025, 1742, 1664, 1624, 1570, 1541, 1492, 1436, 1407, 1341, 1312, 1251, 1228, 1204, 1164, 1135, 1052, 1008, 986, 969, 939, 908, 875, 851, 811, 769, 746, 719, 690, 669, 648, 623, 612, 596, 582, 573, 567, 558 cm^{-1}; ^{1}H NMR (400 MHz, DMSO-d_6): δ 1.87-1.97 (m, 1H, H_A-7), 2.03-2.08 (m, 1H, H_B-7), 2.67-2.75 (m, 3H, H-5, H_A-4), 3.04 (dd, 1H, J_1 = 4.9 Hz, J_2 = 15.2 Hz, H_B-4), 3.58 (s, 2H, $COCH_2CO$), 3.66 (s, 3H, $COOCH_3$), 4.24-4.30 (m, 1H, CHNH), 7.03 (ddd, 1H, J_1 = 1.0 Hz, J_2 = 7.0 Hz, J_3 = 8.0 Hz, Ar-H), 7.15-7.20 (m, 2H, Ar-H), 7.43 (dd, 1H, J_1 = 0.9 Hz, J_2 = 8.2 Hz, Ar-H), 7.61 (dd, 1H, J_1 = 0.8 Hz, J_2 = 7.9 Hz, Ar-H), 8.47 (d, 1H, J = 7.7 Hz, CONHCH), 11.58 (d, 1H, J = 1.6 Hz, NH), 12.15 (s, 1H, NH) ppm; ^{13}C NMR (100 MHz, DMSO-d_6): δ 24.8, 28.4, 28.7, 42.0, 45.5, 52.1, 102.8, 112.3, 119.7, 119.8, 121.5, 123.3, 127.0, 131.6, 136.4, 143.6, 155.1, 160.6, 163.9, 167.6 ppm; HRMS (ESI$^+$) m/z for $C_{20}H_{21}N_4O_4S$ ($[M+H]^+$): calcd 413.1284, found 413.1279; HPLC: t_r 17.800 min (96.5% at 210 nm, 95.8% at 280 nm).

*Methyl (S)-4-((6-(1H-indole-2-carboxamido)-4,5,6,7-tetrahydrobenzo[1,2-d]thiazol-2-yl)amino)-4-oxobutanoate (**30**).* Prepared from **5** (0.250 g, 0.80 mmol) and methyl 4-chloro-4-oxobutanoate (0.147 mL, 1.20 mmol) according to general procedure **F**. Yield: 188 mg (55.0%); off-white crystals; m.p. 202-205 °C; $[\alpha]_D$ +16.9 (*c* 0.27, MeOH); IR (ATR) ν 3350, 3239, 3055, 2950, 2362, 1717, 1666, 1630, 1546, 1492, 1449, 1439, 1418, 1382, 1340, 1313, 1266, 1228, 1208, 1170, 1137, 1107, 1073, 1039, 1008, 987, 971, 932, 911, 897, 870, 845, 824, 809, 799, 782, 767, 742, 685, 604, 584, 574, 561 cm^{-1}; ^1H NMR (400 MHz, DMSO-d_6): δ 1.88-1.98 (m, 1H, H_A-7), 2.05-2.09 (m, 1H, H_B-7), 2.61-2.75 (m, 7H, $COCH_2CH_2CO$, H-5, H_A-4), 3.03 (dd, 1H, J_1 = 4.7 Hz, J_2 = 15.6 Hz, H_B-4), 3.60 (s, 3H, $COOCH_3$), 4.24-4.35 (m, 1H, C<u>H</u>NH), 7.04 (ddd, 1H, J_1 = 1.0 Hz, J_2 = 7.0 Hz, J_3 = 8.0 Hz, Ar-H), 7.16-7.20 (m, 2H, Ar-H), 7.44 (dd, 1H, J_1 = 0.9 Hz, J_2 = 8.2 Hz, Ar-H), 7.62 (dd, 1H, J_1 = 0.8 Hz, J_2 = 7.9 Hz, Ar-H), 8.49 (d, 1H, J = 7.8 Hz, CON<u>H</u>CH), 11.59 (d, 1H, J = 1.5 Hz, NH), 12.00 (s, 1H, NH) ppm; ^{13}C NMR (100 MHz, DMSO-d_6): δ 24.8, 28.0, 28.4, 28.7, 29.7, 45.5, 51.4, 102.8, 112.3, 119.2, 119.7, 121.4, 123.3, 127.0, 131.6, 136.4, 143.4, 155.4, 160.6, 169.7, 172.6 ppm; HRMS (ESI^+) m/z for $C_{21}H_{23}N_4O_4S$ ($[M+H]^+$): calcd 427.1440, found 427.1429; HPLC: t_r 18.257 min (100% at 254 nm).

*Ethyl (S)-2-((6-(4,5-dichloro-1H-pyrrole-2-carboxamido)-4,5,6,7-tetrahydrobenzo[1,2-d]thiazol-2-yl)amino)-2-oxoacetate (**31**).* Prepared from **22** (0.100 g, 0.30 mmol) and ethyl 2-chloro-2-oxoacetate (0.051 mL, 0.45 mmol) according to general procedure **F**. Yield: 25.0 mg (19.2%); yellow crystals; m.p. 140-143 °C; $[\alpha]_D$ -4.2 (*c* 0.21, MeOH); IR (ATR) ν 3125, 2936, 1739, 1696, 1630, 1562, 1519, 1433, 1396, 1369, 1330, 1257, 1230, 1178, 1155, 1115, 1014 cm^{-1}; ^1H NMR (400 MHz, DMSO-d_6): δ 1.31 (t, 3H, J = 7.1 Hz, $CH_2C\underline{H}_3$), 1.83-1.93 (m, 1H, H_A-7), 1.98-2.05 (m, 1H, H_B-7), 2.62-2.80 (m, 3H, H-5, H_A-4), 3.03 (dd, 1H, J_1 = 5.0 Hz, J_2 = 16.1 Hz, H_B-4), 4.17-4.25 (m, 1H, C<u>H</u>NH), 4.29 (q, 2H, J = 7.1 Hz, $C\underline{H}_2CH_3$), 6.98 (s, 1H, Ar-H), 8.14 (d,

1H, *J* = 7.8 Hz, CONHCH), 12.76-12.95 (br s, 1H, 2 × NH) ppm; ^{13}C NMR (100 MHz, DMSO-d_6): δ 13.8, 24.1, 28.3, 28.4, 45.1, 62.4, 100.0, 107.9, 110.0, 114.8, 120.8, 124.8, 158.5 ppm; HRMS (ESI$^+$) m/z for $C_{16}H_{17}Cl_2N_4O_4S$ ([M+H]$^+$): calcd 431.0348, found 431.0336. HPLC: t_r 19.48 min (96.0% at 254 nm).

*Methyl (S)-3-((6-(4,5-dichloro-1H-pyrrole-2-carboxamido)-4,5,6,7-tetrahydrobenzo[1,2-d]thiazol-2-yl)amino)-3-oxopropanoate (**32**).* Prepared from **22** (0.050 g, 0.15 mmol) and methyl 3-chloro-3-oxopropanoate (0.024 mL, 0.23 mmol) according to general procedure **F**. Yield: 24.0 mg (36.9%); yellow crystals; m.p. 136-138 °C; $[\alpha]_D$ +36.8 (*c* 0.20, MeOH); IR (ATR) ν 3172, 2951, 1735, 1627, 1561, 1522, 1434, 1400, 1333, 1253, 1214, 1151, 1080, 1016 cm^{-1}; ^{1}H NMR (400 MHz, DMSO-d_6): δ 1.81-1.92 (m, 1H, H_A-7), 1.96-2.04 (m, 1H, H_B-7), 2.60-2.74 (m, 3H, H-5, H_A-4), 3.00 (dd, 1H, J_1 = 5.1 Hz, J_2 =15.9 Hz, H_B-4), 3.58 (s, 2H, $COCH_2CO$), 3.66 (s, 3H, $COOCH_3$), 4.15-4.24 (m, 1H, CHNH), 6.97 (s, 1H, Ar-H), 8.13 (d, 1H, *J* = 7.6 Hz, CONHCH), 12.15 (s, 1H, NH), 12.75 (s, 1H, NH) ppm; ^{13}C NMR (100 MHz, DMSO-d_6): δ 24.6, 28.4, 28.6, 42.0, 45.2, 52.1, 97.7, 107.9, 109.9, 114.8, 124.8, 143.8, 155.1, 158.5, 163.9, 167.5 ppm; HRMS (ESI$^+$) m/z for $C_{16}H_{17}Cl_2N_4O_4S$ ([M+H]$^+$): calcd 431.0348, found 431.0343. HPLC: t_r 18.58 min (100.0% at 254 nm).

*Methyl (S)-4-((6-(4,5-dichloro-1H-pyrrole-2-carboxamido)-4,5,6,7-tetrahydrobenzo[1,2-d]thiazol-2-yl)amino)-4-oxobutanoate (**33**).* Prepared from **22** (0.250 g, 0.75 mmol) and methyl 4-chloro-4-oxobutanoate (0.126 mL, 0.90 mmol) according to general procedure **F**. Yield: 181.0 mg (53.9%); yellow crystals; m.p. 210-212 °C; $[\alpha]_D$ -5.3 (*c* 0.19, MeOH); IR (ATR) ν 3511, 3185, 3065, 2956, 2853, 1732, 1640, 1585, 1547, 1527, 1438, 1426, 1401, 1371, 1322, 1272, 1206, 1175, 1155, 1113, 1068, 1015, 993, 981, 897, 865, 838, 796, 754, 731, 685, 647, 626, 609 cm^{-1}; ^{1}H NMR (400 MHz, DMSO-d_6): δ 1.80-1.90 (m, 1H, H_A-7), 1.97-2.03 (m, 1H, H_B-7),

2.61-2.70 (m, 7H, H-5, H_A-4, $COCH_2CH_2CO$), 2.98 (dd, 1H, J_1 = 5.0 Hz, J_2 =15.7 Hz, H_B-4), 3.60 (s, 3H, $COOCH_3$), 4.17-4.24 (m, 1H, CHNH), 6.97 (d, 1H, J = 2.7 Hz, Ar-H), 8.11 (d, 1H, J = 7.7 Hz, CONHCH), 11.98 (s, 1H, NH), 12.75 (d, 1H, J = 2.3 Hz, NH) ppm; ^{13}C NMR (100 MHz, DMSO-d_6): δ 24.5, 28.1, 28.3, 28.4, 29.7, 45.3, 51.4, 107.9, 110.0, 114.8, 119.0, 124.8, 143.3, 155.5, 158.5, 169.7, 173.4 ppm; HRMS (ESI^+) m/z for $C_{17}H_{19}Cl_2N_4O_4S$ ($[M+H]^+$): calcd 445.0504, found 445.0499. HPLC: t_r 19.101 min (100.0% at 254 nm).

General procedure **G**. *Synthesis of compounds **34-44***. To a solution of ester (1 mmol) in methanol (5 mL), 1 M NaOH (5 mmol) was added and the reaction mixture stirred at room temperature overnight. Methanol was evaporated under reduced pressure and reaction mixture extracted with ethyl acetate (10 mL). Water phase was acidified with 1 M HCl to pH ~ 2, precipitate was filtered off and purified by flash column chromatography using dichloromethane/methanol (1:1) as eluent.

*(S)-2-((6-(4,5-Dibromo-1H-pyrrole-2-carboxamido)-4,5,6,7-tetrahydrobenzo[1,2-d]thiazol-2-yl)amino)-2-oxoacetic acid (**34**).* Prepared from **23** (0.080 g, 0.15 mmol) according to general procedure **G**. Yield: 66.0 mg (87.2%); yellow crystals; m.p. 229-231 °C; $[\alpha]_D$ +7.1 (*c* 0.19, DMF); IR (ATR) ν 3120, 2934, 1633, 1555, 1515, 1417, 1376, 1301, 1216, 1079 cm^{-1}; ^{1}H NMR (400 MHz, DMSO-d_6): δ 1.82-1.92 (m, 1H, H_A-7), 1.96-2.03 (m, 1H, H_B-7), 2.62-2.79 (m, 3H, H-5, H_A-4), 3.03 (dd, 1H, J_1 = 4.7 Hz, J_2 =15.4 Hz, H_B-4), 4.16-4.26 (m, 1H, CHNH), 7.01 (d, 1H, J = 2.8 Hz, Ar-H), 8.13 (d, 1H, J = 7.9 Hz, CONHCH), 12.72 (d, 1H, J = 2.4 Hz, NH) ppm; ^{13}C NMR (100 MHz, DMSO-d_6): δ 24.5, 28.3, 28.4, 45.0, 97.8, 104.6, 112.9, 128.0, 158.4 ppm; HRMS (ESI^-) m/z for $C_{14}H_{11}Br_2N_4O_4S$ ($[M-H]^-$): calcd 488.8868, found 488.8855; HPLC: t_r 17.45 min (100% at 254 nm).

*(S)-3-((6-(4,5-Dibromo-1H-pyrrole-2-carboxamido)-4,5,6,7-tetrahydrobenzo[1,2-d]thiazol-2-yl)amino)-3-oxopropanoic acid (**35**).* Prepared from **24** (0.202 g, 0.39 mmol) according to general procedure **G**. Yield: 132 mg (67.2%); yellow crystals; m.p. 268 °C (decomposition); $[\alpha]_D$ +38.2 (*c* 0.23, DMF); IR (ATR) ν 3172, 2930, 1556, 1522, 1410, 1326, 1262, 1220, 1161, 1079, 1012 cm^{-1}; ^1H NMR (400 MHz, DMSO-d_6): δ 1.81-1.92 (m, 1H, H_A-7), 1.95-2.04 (m, 1H, H_B-7), 2.62-2.77 (m, 3H, H-5, H_A-4), 2.99 (dd, 1H, J_1 = 5.0 Hz, J_2 =16.1 Hz, H_B-4), 3.46 (s, 2H, $COCH_2CO$), 4.15-4.24 (m, 1H, CHNH), 7.01 (d, 1H, *J* = 1.7 Hz, Ar-H), 8.16 (d, 1H, *J* = 7.7 Hz, CONHCH), 12.09 (br s, 1H, NH), 12.73 (d, 1H, NH) ppm; ^{13}C NMR (100 MHz, DMSO-d_6): δ 24.6, 28.3, 28.5, 42.5, 45.2, 97.7, 104.5, 112.9, 119.5, 128.0, 143.5, 155.2, 158.3, 164.3, 168.6 ppm; HRMS (ESI^+) m/z for $C_{15}H_{15}Br_2N_4O_4S$ ($[M+H]^+$): calcd 504.9181, found 504.9173; HPLC: t_r 18.03 min (100% at 254 nm).

*(S)-4-((6-(4,5-Dibromo-1H-pyrrole-2-carboxamido)-4,5,6,7-tetrahydrobenzo[1,2-d]thiazol-2-yl)amino)-4-oxobutanoic acid (**36**).* Prepared from **25** (0.370 g, 0.69 mmol) according to general procedure **G**. Yield: 340 mg (94.4%); off-white crystals, m.p. 280 °C (decomposition); $[\alpha]_D$ +9.6 (*c* 0.20, DMF); IR (ATR) ν 3173, 2925, 1556, 1409, 1331, 1286, 1285, 1222, 1161, 1079, 1014 cm^{-1}; ^1H NMR (400 MHz, DMSO-d_6): δ 1.80-1.90 (m, 1H, H_A-7), 1.92-1.97 (m, 1H, H_B-7), 2.34 (t, 2H, *J* = 6.4 Hz, $COCH_2$), 2.53-2.69 (m, 5H, H-5, H_A-4, $COCH_2$), 2.89 (dd, 1H, J_1 = 5.1 Hz, J_2 = 15.1 Hz, H_B-4), 4.09-4.17 (m, 1H, CHNH), 6.62 (s, 1H, Ar-H), 7.64 (s, 1H, CONHCH), 12.96 (br s, 1H, NH) ppm; ^{13}C NMR (100 MHz, DMSO-d_6): δ 24.7, 28.7, 28.8, 30.7, 32.9, 44.6, 109.0, 112.4, 114.8, 119.0, 126.4, 143.1, 155.7, 158.5, 171.3, 176.2 ppm; HRMS (ESI^-) m/z for $C_{16}H_{15}Br_2N_4O_4S$ ($[M-H]^-$): calcd 516.9181, found 516.9191; HPLC: t_r 18.086 min (100% at 254 nm).

*(R)-3-((6-(4,5-Dibromo-1H-pyrrole-2-carboxamido)-4,5,6,7-tetrahydrobenzo[1,2-d]thiazol-2-yl)amino)-3-oxopropanoic acid (**37**).* Prepared from **26** (0.020 g, 0.038 mmol) according to general procedure **G**. Yield: 15.0 mg (77.1%); brown crystals; m.p. 192-194 °C; IR (ATR) ν 3388, 3176, 2932, 2846, 1698, 1637, 1556, 1509, 1414, 1391, 1373, 1326, 1217, 1076 cm^{-1}; ^1H NMR (400 MHz, DMSO-d_6): δ 1.81-1.92 (m, 1H, H_A-7), 1.95-2.04 (m, 1H, H_B-7), 2.62-2.77 (m, 3H, H-5, H_A-4), 2.99 (dd, 1H, J_1 = 5.0 Hz, J_2 =16.1 Hz, H_B-4), 3.46 (s, 2H, $COCH_2CO$), 4.15-4.24 (m, 1H, CHNH), 7.01 (d, 1H, J = 1.7 Hz, Ar-H), 8.16 (d, 1H, J = 7.7 Hz, CONHCH), 12.09 (br s, 1H, NH), 12.73 (d, 1H, NH) ppm; ^{13}C NMR (100 MHz, DMSO-d_6): δ 24.6, 28.3, 28.5, 42.5, 45.2, 97.7, 104.5, 112.9, 119.5, 128.0, 143.5, 155.2, 158.3, 164.3, 168.6 ppm; HRMS (ESI^-) m/z for $C_{15}H_{13}Br_2N_4O_4S$ ($[M-H]^-$): calcd 502.9204, found 502.9020; HPLC: t_r 18.077 min (95.1% at 254 nm).

*(S)-3-((6-(4-Bromo-1H-pyrrole-2-carboxamido)-4,5,6,7-tetrahydrobenzo[1,2-d]thiazol-2-yl)amino)-3-oxopropanoic acid (**38**).* Prepared from **27** (0.024 g, 0.054 mmol) according to general procedure **G**. Yield: 14 mg (60.2%); off-white crystals; m.p. 324 °C (decomposition); $[\alpha]_D$ +13.8 (*c* 0.18, DMF); IR (ATR) ν 3280, 2962, 1693, 1614, 1583, 1554, 1515, 1451, 1430, 1406, 1389, 1369, 1328, 1290, 1269, 1235, 1215, 1162, 1127, 1067, 1008 cm^{-1}; ^1H NMR (400 MHz, DMSO-d_6): δ 1.79-1.92 (m, 1H, H_A-7), 1.96-2.05 (m, 1H, H_B-7), 2.59-2.73 (m, 3H, H-5, H_A-4), 2.99 (dd, 1H, J_1 = 4.8 Hz, J_2 = 15.6 Hz, H_B-4), 3.46 (s, 2H, $COCH_2CO$), 4.14-4.25 (m, 1H, CHNH), 6.93 (s, 1H, Ar-H), 7.00 (s, 1H, Ar-H), 8.08 (d, 1H, J = 7.8 Hz, CONHCH), 11.86 (s, 1H, NH/COOH), 12.97 (s, 1H, NH/COOH), 12.79 (d, 1H, J = 2.8 Hz, NH) ppm; ^{13}C NMR (100 MHz, DMSO-d_6): δ 24.6, 28.3, 28.6, 42.4, 45.1, 94.8, 111.6, 119.5, 121.1, 128.7, 143.4, 155.1, 159.0, 164.3, 168.6 ppm; HRMS (ESI^-) m/z for $C_{15}H_{14}BrN_4O_4S$ ($[M-H]^-$): calcd 424.9919, found 424.9910; HPLC: t_r 16.027 min (100% at 254 nm).

*(S)-2-((6-(1H-Indole-2-carboxamido)-4,5,6,7-tetrahydrobenzo[1,2-d]thiazol-2-yl)amino)-2-oxoacetic acid (**39**).* Prepared from **28** (0.187 g, 0.45 mmol) according to general procedure **G**. Yield: 94 mg (53.9%); yellow crystals; m.p. 218-220 °C; $[\alpha]_D$ +23.7 (*c* 0.21, DMF); IR (ATR) ν 2933, 2042, 1691, 1631, 1534, 1436, 1366, 1293, 1267, 1222, 1155, 1082, 1016, 808, 746, 684, 669, 630, 610, 596, 582, 575, 567, 559, 552 cm^{-1}; ^1H NMR (400 MHz, DMSO-d_6): δ 1.90-2.00 (m, 1H, H_A-7), 2.05-2.11 (m, 1H, H_B-7), 2.72-2.81 (m, 3H, H-5, H_A-4), 3.09 (dd, 1H, J_1 = 5.0 Hz, J_2 = 15.5 Hz, H_B-4), 4.25-4.36 (m, 1H, CHNH), 7.04 (ddd, 1H, J_1 = 1.0 Hz, J_2 = 7.0 Hz, J_3 = 8.0 Hz, Ar-H), 7.16-7.21 (m, 2H, Ar-H), 7.44 (dd, 1H, J_1 = 0.9 Hz, J_2 = 8.2 Hz, Ar-H), 7.62 (dd, 1H, J_1 = 0.8 Hz, J_2 = 7.9 Hz, Ar-H), 8.50 (d, 1H, *J* = 7.9 Hz, CONHCH), 11.59 (d, 1H, *J* = 1.8 Hz, NH), 12.54 (br s, 2H, COOH, NH) ppm; ^{13}C NMR (100 MHz, DMSO-d_6): δ 24.6, 28.4, 28.5, 45.4, 102.8, 112.3, 119.7, 120.9, 121.5, 123.3, 127.0, 131.6, 136.4, 160.6, 161.0, 172.0 ppm; HRMS (ESI^+) m/z for $C_{18}H_{17}N_4O_4S$ ($[M+H]^+$): calcd 385.0971, found 385.0981; HPLC: t_r 16.524 min (95.9% at 254 nm).

*(S)-3-((6-(1H-Indole-2-carboxamido)-4,5,6,7-tetrahydrobenzo[1,2-d]thiazol-2-yl)amino)-3-oxopropanoic acid (**40**).* Prepared from **29** (0.063 g, 0.15 mmol) according to general procedure **G**. Yield: 29 mg (47.7%); yellow crystals; m.p. >300 °C; $[\alpha]_D$ +4.5 (*c* 0.20, DMF); IR (ATR) ν 3184, 3066, 2956, 2853, 2359, 1732, 1676, 1639, 1545, 1527, 1438, 1426, 1401, 1371, 1322, 1271, 1225, 1206, 1175, 1156, 1113, 1075, 1017, 993, 981, 897, 865, 839, 812, 796, 748, 685, 626, 612, 603, 587 cm^{-1}; ^1H NMR (400 MHz, DMSO-d_6): δ 1.88-1.98 (m, 1H, H_A-7), 2.03-2.10 (m, 1H, H_B-7), 2.67-2.76 (m, 3H, H-5, H_A-4), 3.05 (dd, 1H, J_1 = 5.3 Hz, J_2 = 15.1 Hz, H_B-4), 3.46 (s, 2H, $COCH_2CO$), 4.27-4.33 (m, 1H, CHNH), 7.04 (ddd, 1H, J_1 = 1.0 Hz, J_2 = 7.0 Hz, J_3 = 8.0 Hz, Ar-H), 7.16-7.20 (m, 2H, Ar-H), 7.44 (dd, 1H, J_1 = 0.8 Hz, J_2 = 8.2 Hz, Ar-H), 7.62 (dd, 1H, J_1 = 0.7 Hz, J_2 = 8.0 Hz, Ar-H), 8.48 (d, 1H, *J* = 7.8 Hz, CONHCH), 11.59 (d, 1H, *J* = 1.7

Hz, NH), 12.08 (br s, 1H, NH/COOH), 12.79 (br s, 1H, NH/COOH) ppm; ^{13}C NMR (100 MHz, DMSO-d_6): δ 24.9, 28.3, 28.7, 42.4, 45.6, 103.2, 112.2, 119.6, 121.4, 123.2, 127.0, 131.4, 136.4, 143.5, 155.2, 160.5, 164.6, 168.7 ppm; HRMS (ESI$^+$) m/z for $C_{19}H_{19}N_4O_4S$ ([M+H]$^+$): calcd 399.1127, found 399.1126; HPLC: t_r 16.754 min (100% at 254 nm).

*(S)-4-((6-(1H-Indole-2-carboxamido)-4,5,6,7-tetrahydrobenzo[1,2-d]thiazol-2-yl)amino)-4-oxobutanoic acid (**41**).* Prepared from **30** (0.173 g, 0.41 mmol) according to general procedure **G**. Yield: 106 mg (63.4%); white crystals; m.p. 225-227 °C; $[\alpha]_D$ +17.6 (*c* 0.17, DMF); IR (ATR) ν 3283, 2943, 2363, 1744, 1660, 1577, 1536, 1480, 1456, 1405, 1374, 1350, 1302, 1276, 1247, 1203, 1165, 1124, 1096, 1028, 1008, 987, 969, 929, 877, 845, 812, 745, 736, 669, 648, 611, 589, 582, 575, 563, 559 cm^{-1}; ^{1}H NMR (400 MHz, DMSO-d_6): δ 1.88-1.98 (m, 1H, H_A-7), 2.05-2.09 (m, 1H, H_B-7), 2.53-2.74 (m, 7H, H-5, H_A-4, $COCH_2CH_2CO$), 3.03 (dd, 1H, J_1 = 5.2 Hz, J_2 = 15.3 Hz, H_B-4), 4.24-4.33 (m, 1H, C<u>H</u>NH), 7.04 (ddd, 1H, J_1 = 1.0 Hz, J_2 = 7.0 Hz, J_3 = 8.0 Hz, Ar-H), 7.16-7.20 (m, 2H, Ar-H), 7.44 (dd, 1H, J_1 = 0.9 Hz, J_2 = 8.2 Hz, Ar-H), 7.62 (dd, 1H, J_1 = 0.7 Hz, J_2 = 7.9 Hz, Ar-H), 8.47 (d, 1H, *J* = 7.8 Hz, CON<u>H</u>CH), 11.58 (d, 1H, *J* = 1.9 Hz, NH), 11.96 (s, 1H, NH/COOH), 12.19 (br s, 1H, NH/COOH) ppm; ^{13}C NMR (100 MHz, DMSO-d_6): δ 24.8, 28.3, 28.4, 28.7, 29.8, 45.5, 102.8, 112.3, 119.1, 119.7, 121.4, 123.3, 127.0, 131.6, 136.4, 143.4, 155.5, 160.6, 169.9, 173.6 ppm; HRMS (ESI$^+$) m/z for $C_{20}H_{21}N_4O_4S$ ([M+H]$^+$): calcd 413.1284, found 413.1284; HPLC: t_r 16.990 min (100% at 254 nm).

*(S)-2-((6-(4,5-Dichloro-1H-pyrrole-2-carboxamido)-4,5,6,7-tetrahydrobenzo[1,2-d]thiazol-2-yl)amino)-2-oxoacetic acid (**42**).* Prepared from **31** (0.161 g, 0.37 mmol) according to general procedure **G**. Yield: 99 mg (66.0%); yellow crystals; m.p. 183-185 °C; $[\alpha]_D$ +6.7 (*c* 0.23, DMF); IR (ATR) ν 3735, 3164, 2949, 2361, 2342, 2175, 2014, 1977, 1739, 1719, 1686, 1654, 1624, 1566, 1522, 1436, 1400, 1332, 1265, 1219, 1162, 1083, 1018, 987, 920, 875, 844, 811, 767, 748,

669, 654, 638, 624, 616, 605, 590, 582, 575, 566, 559 cm^{-1}; ^1H NMR (400 MHz, DMSO-d_6): δ 1.85-1.93 (m, 1H, H_A-7), 1.98-2.04 (m, 1H, H_B-7), 2.63-2.75 (m, 3H, H-5, H_A-4), 3.04 (dd, 1H, J_1 = 5.3 Hz, J_2 =15.6 Hz, H_B-4), 4.17-4.26 (m, 1H, CHNH), 6.98 (d, 1H, J = 2.9 Hz, Ar-H), 8.15 (d, 1H, J = 7.7 Hz, CONHCH), 12.76 (d, 1H, J = 2.8 Hz, NH) ppm; ^{13}C NMR (100 MHz, DMSO-d_6): δ 24.4, 28.3, 28.4, 45.1, 95.2, 107.9, 110.0, 114.8, 120.8, 124.8, 147.5, 158.5, 161.0 ppm; HRMS (ESI^+) m/z for $C_{14}H_{13}Cl_2N_4O_4S$ ($[M+H]^+$): calcd 403.0035, found 403.0044; HPLC: t_r 17.036 min (95.2% at 254 nm, 98.1% at 210 nm).

*(S)-3-((6-(4,5-Dichloro-1H-pyrrole-2-carboxamido)-4,5,6,7-tetrahydrobenzo[1,2-d]thiazol-2-yl)amino)-3-oxopropanoic acid (**43**).* Prepared from **32** (0.177 g, 0.11 mmol) according to general procedure **G**. Yield: 94 mg (55.3%); off-white solid; m.p. >300 °C; $[\alpha]_D$ +1.7 (*c* 0.23, DMF); IR (ATR) ν 2043, 2025, 1928, 1736, 1686, 1624, 1561, 1523, 1438, 1400, 1333, 1262, 1220, 1161, 1082, 1017, 919, 874, 843, 810, 765, 748, 669, 657, 623, 615, 591, 583, 574, 559 cm^{-1}; ^1H NMR (400 MHz, DMSO-d_6): δ 1.81-1.91 (m, 1H, H_A-7), 1.97-2.03 (m, 1H, H_B-7), 2.62-2.73 (m, 3H, H-5, H_A-4), 3.00 (dd, 1H, J_1 = 5.3 Hz, J_2 = 15.6 Hz, H_B-4), 3.46 (s, 2H, $COCH_2CO$), 4.15-4.24 (m, 1H, CHNH), 6.97 (d, 1H, J = 2.9 Hz, Ar-H), 8.13 (d, 1H, J = 7.8 Hz, CONHCH), 12.07 (s, 1H, NH), 12.73 (d, 1H, J = 2.8 Hz, NH) ppm; ^{13}C NMR (100 MHz, DMSO-d_6): δ 24.6, 28.3, 28.5, 42.4, 45.2, 107.8, 109.9, 114.8, 119.4, 124.7, 143.5, 155.2, 158.4, 164.3, 168.6 ppm; HRMS (ESI^-) m/z for $C_{15}H_{15}Cl_2N_4O_4S$ ($[M+H]^+$): calcd 417.0186, found 417.0182; HPLC: t_r 17.739 min (95.1% at 254 nm).

*(S)-4-((6-(4,5-Dichloro-1H-pyrrole-2-carboxamido)-4,5,6,7-tetrahydrobenzo[1,2-d]thiazol-2-yl)amino)-4-oxobutanoic acid (**44**).* Prepared from **33** (0.170 g, 0.31 mmol) according to general procedure **G**. Yield: 85 mg (63.0%); white crystals, m.p. 252-253 °C; $[\alpha]_D$ +5.2 (*c* 0.18, DMF); IR (ATR) ν 3418, 2984, 2941, 2361, 1655, 1578, 1496, 1456, 1438, 1403, 1373, 1355, 1303,

1240, 1204, 1166, 1096, 1010, 987, 970, 928, 878, 844, 811, 761, 715, 686, 669, 650, 629, 612, 590, 571, 559 cm^{-1}; ^1H NMR (400 MHz, DMSO-d_6): δ 1.80-1.90 (m, 1H, H_A-7), 1.95-2.01 (m, 1H, H_B-7), 2.53-2.71 (m, 7H, H-5, H_A-4, $COCH_2CH_2CO$), 2.98 (dd, 1H, J_1 = 5.3 Hz, J_2 = 15.7 Hz, H_B-4), 4.14-4.24 (m, 1H, CHNH), 6.97 (d, 1H, J = 2.9 Hz, Ar-H), 8.12 (d, 1H, J = 7.8 Hz, CONHCH), 11.95 (s, 1H, NH/COOH), 12.20 (s, 1H, NH/COOH), 12.75 (d, 1H, J = 2.7 Hz, NH) ppm; ^{13}C NMR (100 MHz, DMSO-d_6): δ 24.7, 28.3, 28.4, 28.6, 29.8, 45.3, 107.9, 109.9, 114.8, 119.0, 124.8, 143.3, 155.5, 158.5, 169.9, 173.6 ppm; HRMS (ESI^+) m/z for $C_{16}H_{17}Cl_2N_4O_4S$ ($[M+H]^+$): calcd 431.0348, found 431.0352; HPLC: t_r 18.086 min (97.5% at 254 nm, 100% at 210 nm).

*(S)-N-(2-Acetamido-4,5,6,7-tetrahydrobenzo[1,2-d]thiazol-6-yl)-4,5-dibromo-1H-pyrrole-2-carboxamide (**45**).* Prepared from **3** (0.070g, 0.166mmol) and acetyl chloride (0.018 mL, 0.25 mmol) according to general procedure **F**. Yield: 56.0 mg (72.7%); yellow crystals; m.p. 288 °C (decomposition); $[\alpha]_D$ +8.4 (*c* 0.18, MeOH); IR (ATR) ν 3366, 3177, 3059, 2935, 2845, 1672, 1637, 1553, 1518, 1415, 1367, 1329, 1290, 1270, 1220, 1106, 1078, 1038, 1001 cm^{-1}; ^1H NMR (400 MHz, DMSO-d_6): δ 1.79-1.93 (m, 1H, H_A-7), 1.95-2.04 (m, 1H, H_B-7), 2.60-2.77 (m, 3H, H-5, H_A-4), 3.00 (dd, 1H, J_1 = 5.7 Hz, J_2 =15.5 Hz, H_B-4), 3.66 (s, 3H, $COCH_3$), 4.15-4.24 (m, 1H, CHNH), 7.01 (s, 1H, Ar-H), 8.11 (d, 1H, J = 7.0 Hz, CONHCH), 12.15 (s, 1H, NH), 12.71 (s, 1H, NH) ppm; ^{13}C NMR (100 MHz, DMSO-d_6): δ 24.6, 28.3, 28.6, 30.7, 45.2, 97.7, 104.5, 112.9, 119.3, 128.0, 143.4, 155.2, 158.3, 167.9 ppm; HRMS (ESI^-) m/z for $C_{14}H_{14}Br_2N_4O_2S$ ($[M-H]^-$): calcd 458.9126, found 458.9118; HPLC: t_r 18.61 min (100% at 254 nm).

*(S)-4,5-Dibromo-N-(2-oxo-3,4,6,7,8,9-hexahydro-2H-benzo[4,5]thiazolo[3,2-a]pyrimidin-8-yl)-1H-pyrrole-2-carboxamide (**46**).* Compound **3** (0.050 g, 0.12 mmol) and Na_2CO_3 (0.028 g, 0.26 mmol) were suspended in dry acetonitrile (0.750 mL), and then the suspension was cooled

to 0 °C. A 1 M solution of acryloyl chloride (0.143 mL, 0.14 mmol) in dry acetonitrile was then added drop wise, and the resulting reaction mixture was stirred at 0 °C for 2 h. Sodium iodide (0.018 g, 0.12 mmol) was then added and the reaction mixture was heated to 80 °C for 24 h. The reaction mixture was concentrated under reduced pressure, diluted with water, and extracted with dichloromethane. The combined organic phases were washed, dried over Na_2SO_4, filtered and concentrated under reduced pressure. Crude product was purified by flash column chromatography using dichloromethane/methanol (9:1) as eluent. Yield: 21 mg (37.2%); yellow crystals; m.p. 286 °C (decomposition); $[\alpha]_D$ +17.4 (*c* 0.22, MeOH); IR (ATR) ν 3419, 3274, 3184, 2939, 1633, 1558, 1494, 1448, 1410, 1362, 1260, 1222, 1081, 1054, 1019 cm^{-1}; ^1H NMR (400 MHz, CD_3OD) δ 1.93-2.02 (m, 1H, H_A-7), 2.14-2.19 (m, 1H, H_B-7), 2.62-2.73 (m, 5H, H-5, H_A-4, CH_2), 2.96 (d, 1H, *J* = 15.8 Hz, H_B-4), 4.14 (t, 2H, *J* = 7.3 Hz, CH_2), 4.28-4.38 (m, 1H, CHNH), 6.91 (s, 1H, Ar-H), ppm; ^{13}C NMR (100 MHz, DMSO-d_6) δ 20.6, 23.5, 27.1, 28.4, 28.8, 40.7, 43.3, 110.9, 111.0, 112.3, 132.4, 133.2, 135.0, 175.0 ppm; HRMS (ESI^-) m/z for $C_{15}H_{14}Br_2N_4O_2S$ ($[M-H]^-$): calcd 470.9126, found 470.9121; HPLC: t_r 14.73 min (100% at 254 nm).

*(S)-N^1-(6-(4,5-Dibromo-1H-pyrrole-2-carboxamido)-4,5,6,7-tetrahydrobenzo[1,2-d]thiazol-2-yl)malonamide (**47**).* To a solution of **24** (0.060 g, 0.12 mmol) in ethanol (2 mL), gas ammonia was bubbled for 2 h. Solvent was removed *in vacuo* and crude product purified by flash column chromatography using dichloromethane/methanol (9:1) as eluent. Yield: 20 mg (34.3%); off-white solid; m.p. 148-151 °C; $[\alpha]_D$ +19.4 (*c* 0.17, MeOH); IR (ATR) ν 3173, 2934, 1658, 1625, 1552, 1519, 1412, 1389, 1326, 1263, 1217, 1150, 1099, 1011 cm^{-1}; ^1H NMR (400 MHz, DMSO-d_6): δ 1.80-1.92 (m, 1H, H_A-7), 1.96-2.04 (m, 1H, H_B-7), 2.59-2.72 (m, 3H, H-5, H_A-4), 2.98 (dd, 1H, J_1 = 5.5 Hz, J_2 =15.5 Hz, H_B-4), 3.32 (s, 2H, $COCH_2CO$), 4.14-4.25 (m, 1H, CHNH), 7.01

(s, 1H, Ar-H), 7.18 (s, 1H, $CONH_2$-H_A), 7.56 (s, 1H, $CONH_2$-H_B), 8.12 (d, 1H, J = 7.2 Hz, CONHCH), 11.98 (s, 1H, NH), 12.71 (s, 1H, NH) ppm; ^{13}C NMR (100 MHz, DMSO-d_6): δ 24.6, 28.4, 28.6, 42.9, 45.2, 97.7, 104.5, 112.9, 119.3, 128.0, 143.5, 155.2, 158.4, 165.5, 168.0 ppm; HRMS (ESI^+) m/z for $C_{15}H_{15}Br_2N_5O_3S$ ($[M+H]^+$): calcd 503.9341, found 503.9351; HPLC: t_r 17.31 min (100% at 254 nm).

***In vitro* Inhibitory Activity Screening and Determination of IC_{50} Values on *E. coli* and *S. aureus* Gyrase.** The assay for determining IC_{50} values (Inspiralis) was performed on black streptavidin-coated 96-well microtiter plates (Thermo Scientific Pierce). The plate was first rehydrated with the wash buffer supplied (20 mM Tris-HCl (pH 7.6), 137 mM NaCl, 0.01% (w/v) BSA, 0.05% (v/v) Tween 20). Biotinylated oligonucelotide was immobilized onto the wells. The excess of oligonucleotide was then washed off and the enzyme assay carried out in the wells. The final reaction volume of 30 μL in buffer (35 mM Tris HCl pH 7.5; 24 mM KCl; 4 mM $MgCl_2$; 2 mM DTT; 1.8 mM spermidine; 1 mM ATP; 6.5 % (w/v) glycerol; 0.1 mg/mL albumin) contained 1.5 U of DNA gyrase from *E. coli* or *S. aureus*, 0.75 μg of relaxed pNO1 plasmid, and 3 μL of inhibitors solution in 10% DMSO and 0.008% Tween® 20. Reactions were incubated for 30 min at 37 °C and, after addition of the TF buffer (50 mM NaOAc pH 5.0, 50 mM NaCl and 50 mM $MgCl_2$), which terminated the enzymatic reaction, for another 30 min at room temperature to allow triplex formation (biotin−oligonucleotide−plasmid). The unbound plasmid was then washed off using TF buffer, and a solution of SybrGOLD stain in T10 buffer (10 mM Tris × HCl pH 8.0 and 1 mM EDTA) was added. After mixing, the fluorescence (excitation, 485 nm; emission, 535 nm) was read using a BioTek's Synergy H4 microplate reader. Preliminary screening was performed at inhibitor concentrations of 100 μM and 10 μM. For the most potent compounds IC_{50} was determined with 7 concentrations of the inhibitors. IC_{50}

values were calculated using GraphPad Prism software and represent the concentration of inhibitor where the residual activity of the enzyme is 50% in three independent measurements; the final result is given as their average value. Novobiocin (IC_{50} = 0.17 μM (lit. 0.08 μM[44]) for *E. coli* DNA gyrase and IC_{50} = 0.041 μM (lit. 0.01 μM[44]) for *S. aureus* DNA gyrase) was used as a positive control.

In vitro **Inhibitory Activity Screening and Determination of IC_{50} Values on *E. coli* and *S. aureus* topoisomerase IV.** The assay for the determination of IC_{50} values (Inspiralis) was performed on the black streptavidin-coated 96-well microtiter plates (Thermo Scientific Pierce). The plate was first rehydrated with the supplied wash buffer (20 mM Tris-HCl (pH 7.6), 137 mM NaCl, 0.01% (w/v) BSA, 0.05% (v/v) Tween® 20) and biotinylated oligonucelotide was immobilized onto the wells. The excess of oligonucleotide was then washed off, and the enzyme assay carried out in the wells. The final reaction volume of 30 μL in buffer (40 mM HEPES KOH (pH 7.6), 100 mM potassium glutamate, 10 mM magnesium acetate, 10 mM DTT, 1 mM ATP, 0.05 mg/mL albumin) contained 1.5 U of topoisomerase IV from *E. coli* or *S. aureus*, 0.75 μg of supercoiled pNO1 plasmid, and 3 μL of inhibitors solution in 10% DMSO and 0.008% Tween 20. Reactions were incubated for 30 min at 37 °C, and after addition of the TF buffer (50 mM NaOAc pH 5.0, 50 mM NaCl and 50 mM $MgCl_2$), which terminated the enzymatic reaction, for another 30 min at room temperature to allow triplex formation (biotin−oligonucleotide−plasmid). The unbound plasmid was then washed off using TF buffer and the solution of SybrGOLD stain in T10 buffer (10 mM Tris-HCl pH 8.0 and 1 mM EDTA) was added. After mixing, fluorescence (excitation, 485 nm; emission, 535 nm) was read using a BioTek's Synergy H4 microplate reader. Preliminary screening was performed at inhibitor concentrations of 100 μM and 10 μM. For most potent compounds IC_{50} was determined with 7

concentrations of the inhibitors. IC_{50} values were calculated using GraphPad Prism software and represent the concentration of inhibitor where the residual activity of the enzyme is 50% in three independent measurements; the final result is given as their average value. Novobiocin (IC_{50} = 11 μM (lit. 10 μM[44]) for *E. coli* topoisomerase IV and IC_{50} = 27 μM (lit. 20 μM[44]) for *S. aureus* topoisomerase IV) was used as a positive control.

***Escherichia coli* DNA gyrase ATPase assay**. Compounds were diluted in DMSO and water to give 2 mM concentration in 50% DMSO, then serially diluted in 50% DMSO/water. 10 μL was added to a final assay volume of 100 μL giving a final DMSO concentration in the assays of 5% (v/v). Compounds were tested between either 200 and 0.005 μM or 25 and 0.0001 μM. Controls also contained a final concentration of 5% DMSO.

E. coli gyrase ATPase activity (Inspiralis) was measured in a linked assay which follows the hydrolysis of ATP via the conversion of NADH to NAD+. *E. coli* DNA gyrase (10 μL of 500 nM) was incubated at 25 °C in a final volume of 100 μL containing 1X assay buffer (50 mM Tris.HCl (pH 7.5), 1 mM EDTA, 5 mM $MgCl_2$, 5 mM DTT, 10% (w/v) glycerol)), 800 μM phosphoenolpyruvate, 400 μM NADH, 1.5 μL phosphokinase/lactate dehydrogenase (PK/LDH) enzyme mix, 0.36 μM linear pBR322 plus or minus inhibitors. The order of addition to the wells was buffer/water/DNA mix, then compounds and then the enzyme. This was equilibrated and the A340 measured for 10 mins at 25 °C. Reactions were then initiated by the addition of ATP (Mg^{2+}) to 2 mM and the decrease in A340 measured over time.

Raw data were collected as a change in OD340 with time (values quoted as milli OD340/min) and converted to a % of the 100% control (enzyme in the absence of inhibitors) after subtraction of the background (no enzyme) rate. These were analyzed using SigmaPlot Version 12.5 (2014).

Determination of Antibacterial Activity. Antimicrobial assays were performed by the broth microdilution method following the guidelines of the Clinical and Laboratory Standards Institute (CLSI; Methods for dilution antimicrobial susceptibility tests for bacteria that grow aerobically, Approved standards – Ninth Edition; M07-A9, Vol.32 No.2). Primarily the following CLSI recommended quality control strains for susceptibility testing were used in the antibacterial assays: *Enterococcus faecalis* (Gram positive, ATCC 29212), *Staphylococcus aureus* (Gram positive, ATCC 25923), *Escherichia coli* (Gram negative, ATCC 25922) and *Pseudomonas aeruginosa* (Gram negative, ATCC 27853). In addition, *E. coli* tolC::Tn10, efflux deficient strain lacking functional tolC gene, and *E. coli* imp4213::Tn10 strain with altered permeability of the outer membrane, were used. Primary screening of compounds against the ATCC strains was initially carried out at a final concentration of 50 μM (n = 3). Compounds that showed >50% inhibition in the primary screen were tested further at several concentrations to confirm the activity and to determine MIC values. The compounds were further assayed against the *E. coli* strains in ten 2-fold dilutions starting from 256 μg/mL concentration. Azithromycin (USP, Cat. 1046056), ciprofloxacin (USP, Cat. 1134313 or ICN Biomedicals, Inc.) and meropenem (USP, Cat. 1392454) were used as standard antibiotics.

Surface Plasmon Resonance (SPR) Measurements. Surface plasmon resonance (SPR) measurements for compounds were performed on a BiacoreX machine using CM5 sensor chip (Biacore, GE Healthcare). The system was primed twice with running buffer (10 mM Hepes pH 7.4, 150 mM NaCl, 3 mM EDTA, 0.005% surfactant P20). The G24 protein was immobilized on the second flow cell of a sensor chip CM5 using the standard amino coupling method. Briefly, the carboxymethylated dextran layer was activated with a 7 min pulse of 1-ethyl-3-(3-dimethylaminopropyl)-carbodiimide (EDC) and *N*-hydroxysuccinimide (NHS) mixed in a 1:1

ratio. Protein was diluted to the final concentration of 50 μg/mL in 10 mM sodium acetate (pH = 4.5) and injected in two short pulses to reach the final immobilization level around 17400 response units. Finally, the rest of the surface was deactivated with a 7 min injection of ethanolamine. The first flow cell was activated with EDC/NHS and deactivated with ethanolamine and served as a reference cell for subtraction of nonspecific binding. Analytes were prepared as DMSO 100× stock solutions and were diluted with a running buffer prior to the injection. They were injected at a flow rate of 30 μL/min for 90 s, and dissociation was monitored for an additional 120 s. Since the dissociation of analytes from the ligand was rapid, no regeneration protocol was needed. For the titration of analytes, the 1% of the DMSO was added to the running buffer in order to diminish the difference in refractive index between the samples and running buffer. Selected compounds **3**, **24**, **25**, **32**, **35**, **36** and **43** were tested at at least eight different concentrations (depending on their solubility) in three parallel titrations. Some of the concentrations were injected several times to check for the reproducibility of the binding. The sensorgrams (Figure S2) were analyzed using BiaEval software (Biacore, GE Healthcare). Equilibrium binding responses were determined from the binding levels 5 s before the stop of the injection. K_d values were determined by fitting of the data to a 1:1 steady state binding model as described in results.

Molecular Modeling.

***Ligand and Protein Preparation*.** Three-dimensional models of designed compounds were built in ChemBio3D Ultra 13.0.[45] Their geometries were optimized using MMFF94[46] force field and partial atomic charges were added. Energy was minimized until the gradient value was smaller than 0.001 kcal/(mol Å). The optimized structure was further refined with GAMESS interface in ChemBio3D Ultra 13.0 using the semiempirical PM3 method, QA optimization algorithm and

Gasteiger Hückel charges for all atoms for 100 steps.[46] Molecular docking calculations were performed using FlexX,[41,42] as available in LeadIT,[43] running on four octal core AMD Opteron CPU processors, 16 GB RAM, two 750 GB hard drives, running 64-bit Scientific Linux 6.0. Receptor was prepared in a LeadIT graphical user interface using the Receptor wizard. Amino acid residues within a radius of 7 Å around the ligand from the X-ray structure (PDB entry: 4DUH[29]) were defined as the binding site. Hydrogen atoms were added to the binding site residues and correct tautomers and protonation states were assigned. Water molecules, except HOH614, and the ligand were deleted from the crystal structure.

Validation of the Docking Protocol and Ligand Docking. The FlexX molecular docking program, as available in LeadIT,[43] was used for ligand docking. A hybrid algorithm (enthalpy and entropy driven ligand binding) was used to place the 'base fragment'. The maximum number of solutions per iteration and the maximum number of solutions per fragmentation parameter values were increased to 1000, while other parameters were set at their default values.

In order to validate our docking protocol, crystal structure ligand was docked into the defined ATP-binding site of *E. coli* GyrB using the above described docking parameters. The protocol was able to reproduce the binding of the crystal structure ligand with an RMSD value of 1.2 Å, which highlights the docking protocol as suitable for binding mode studies of the designed DNA gyrase inhibitors, which were docked using the same settings as used for docking protocol validation. Proposed binding modes and scoring function scores of the top five highest scored docking poses per ligand were evaluated and the highest ranked binding pose was used for graphical representation in PyMOL.[31]

Screening against PAINS. To evaluate a library of the synthesized compounds against PAINS,[47] all tested compounds were screened against the PAINS filter using Python script filter_pains.py, downloaded from GitHub (https://github.com/Team-SKI/snippets/blob/1d1d0424ba15da08cdc7e18c9a27d55b1a6cb797/Python/filter_pains.py). All compounds passed the PAINS filter.

ASSOCIATED CONTENT

Supporting Information. Synthesis of (*S*)-**18** and (*R*)-**18**, primary antibacterial activity screening results and SPR sensorgrams. This material is available free of charge via the Internet at http://pubs.acs.org.

AUTHOR INFORMATION

Corresponding Author

*To whom correspondence should be addressed. Phone: +386-1-4769561; Fax: +386-1-4258031; e-mail: danijel.kikelj@ffa.uni-lj.si

Author Contributions

The manuscript was written through contributions of all authors. All authors have given approval to the final version of the manuscript. ‡These authors contributed equally.

ACKNOWLEDGMENT

This work was supported by the Slovenian Research Agency (Grant No. P1-0208) and by the EU FP7 Project MAREX: Exploring Marine Resources for Bioactive Compounds: From Discovery to Sustainable Production and Industrial Applications (Project No. FP7-KBBE-2009-3-245137). Sotirios Katsamakas is also thankful to ”CMEPIUS Center of the Republic of Slovenia for

Mobility and European Educational and Training Programmes" and "The A. G. Leventis Foundation" for financial support. The authors thank Nicolas Burton (Inspiralis) for performing the ATPase assay. The authors thank Dr. Dušan Žigon (Mass Spectrometry Center**,** Jožef Stefan Institute, Ljubljana, Slovenia) for recording mass spectra. The authors thank Roger Pain for proofreading the manuscript.

ABBREVIATIONS

DMF, *N,N*-dimethylformamide; Gyr A, DNA gyrase subunit A; GyrB, DNA gyrase subunit B; ParC, topoisomerase IV subunit C; HepG2, human hepatocellular carcinoma cell line; ParE, topoisomerase IV subunit E; RA, residual activity; SAR, structure-activity relationship; SPR, surface plasmon resonance; TBTU, *O*-(benzotriazol-1-yl)-*N*,*N*,*N*′,*N*′-tetramethyluronium tetrafluoroborate; THP-1, acute monocytic leukaemia cell line.

REFERENCES

(1) Boucher, H. W.; Talbot, G. H.; Bradley, J. S.; Edwards, J. E.; Gilbert, D.; Rice, L. B.; Scheld, M.; Spellberg, B.; Bartlett, J. Bad bugs, no drugs: no ESKAPE! An update from the Infectious Diseases Society of America. *Clin. Infect. Dis.* **2009**, *48*, 1-12.

(2) Silver, L. L. Challenges of antibacterial discovery. *Clin. Microbiol. Rev.* **2011**, *24*, 71-109.

(3) Collin, F.; Karkare, S.; Maxwell, A. Exploiting bacterial DNA gyrase as a drug target: current state and perspectives. *Appl. Microbiol. Biotechnol.* **2011**, *92*, 479-497.

(4) Sissi, C.; Palumbo, M. In front of and behind the replication fork: bacterial type IIA topoisomerases. *Cell Mol. Life Sci.* **2010**, *67*, 2001-2024.

(5) Champoux, J. J. DNA topoisomerases: structure, function, and mechanism. *Annu. Rev. Biochem.* **2001**, *70*, 369-413.

(6) Emmerson, A. M.; Jones, A. M. The quinolones: decades of development and use. *J. Antimicrob. Chemother.* **2003**, *51 Suppl 1*, 13-20.

(7) Oblak, M.; Kotnik, M.; Šolmajer, T. Discovery and development of ATPase inhibitors of DNA gyrase as antibacterial agents. *Curr. Med. Chem.* **2007**, *14*, 2033-2047.

(8) Drlica, K.; Malik, M. Fluoroquinolones: action and resistance. *Curr. Top. Med. Chem.* **2003**, *3*, 249-282.

(9) Sanyal, G.; Doig, P. Bacterial DNA replication enzymes as targets for antibacterial drug discovery. *Expert Opin. Drug Discov.* **2012**, *7*, 327-339.

(10) Tomašić, T.; Mašič, L. P. Prospects for developing new antibacterials targeting bacterial type IIA topoisomerases. *Curr. Top. Med. Chem.* **2014**, *14*, 130-151.

(11) Ronkin, S. M.; Badia, M.; Bellon, S.; Grillot, A. L.; Gross, C. H.; Grossman, T. H.; Mani, N.; Parsons, J. D.; Stamos, D.; Trudeau, M.; Wei, Y.; Charifson, P. S. Discovery of pyrazolthiazoles as novel and potent inhibitors of bacterial gyrase. *Bioorg. Med. Chem. Lett.* **2010**, *20*, 2828-2831.

(12) Manchester, J. I.; Dussault, D. D.; Rose, J. A.; Boriack-Sjodin, P. A.; Uria-Nickelsen, M.; Ioannidis, G.; Bist, S.; Fleming, P.; Hull, K. G. Discovery of a novel azaindole class of antibacterial agents targeting the ATPase domains of DNA gyrase and topoisomerase IV. *Bioorg. Med. Chem. Lett.* **2012**, *22*, 5150-5156.

(13) Tari, L. W.; Trzoss, M.; Bensen, D. C.; Li, X.; Chen, Z.; Lam, T.; Zhang, J.; Creighton, C. J.; Cunningham, M. L.; Kwan, B.; Stidham, M.; Shaw, K. J.; Lightstone, F. C.; Wong, S. E.; Nguyen, T. B.; Nix, J.; Finn, J. Pyrrolopyrimidine inhibitors of DNA gyrase B (GyrB) and

topoisomerase IV (ParE). Part I: Structure guided discovery and optimization of dual targeting agents with potent, broad-spectrum enzymatic activity. *Bioorg. Med. Chem. Lett.* **2013**, *23*, 1529-1536.

(14) Trzoss, M.; Bensen, D. C.; Li, X.; Chen, Z.; Lam, T.; Zhang, J.; Creighton, C. J.; Cunningham, M. L.; Kwan, B.; Stidham, M.; Nelson, K.; Brown-Driver, V.; Castellano, A.; Shaw, K. J.; Lightstone, F. C.; Wong, S. E.; Nguyen, T. B.; Finn, J.; Tari, L. W. Pyrrolopyrimidine inhibitors of DNA gyrase B (GyrB) and topoisomerase IV (ParE), Part II: development of inhibitors with broad spectrum, Gram-negative antibacterial activity. *Bioorg. Med. Chem. Lett.* **2013**, *23*, 1537-1543.

(15) Starr, J. T.; Sciotti, R. J.; Hanna, D. L.; Huband, M. D.; Mullins, L. M.; Cai, H.; Gage, J. W.; Lockard, M.; Rauckhorst, M. R.; Owen, R. M.; Lall, M. S.; Tomilo, M.; Chen, H.; McCurdy, S. P.; Barbachyn, M. R. 5-(2-Pyrimidinyl)-imidazo[1,2-*a*]pyridines are antibacterial agents targeting the ATPase domains of DNA gyrase and topoisomerase IV. *Bioorg. Med. Chem. Lett.* **2009**, *19*, 5302-5306.

(16) Charifson, P. S.; Grillot, A. L.; Grossman, T. H.; Parsons, J. D.; Badia, M.; Bellon, S.; Deininger, D. D.; Drumm, J. E.; Gross, C. H.; LeTiran, A.; Liao, Y.; Mani, N.; Nicolau, D. P.; Perola, E.; Ronkin, S.; Shannon, D.; Swenson, L. L.; Tang, Q.; Tessier, P. R.; Tian, S. K.; Trudeau, M.; Wang, T.; Wei, Y.; Zhang, H.; Stamos, D. Novel dual-targeting benzimidazole urea inhibitors of DNA gyrase and topoisomerase IV possessing potent antibacterial activity: intelligent design and evolution through the judicious use of structure-guided design and structure-activity relationships. *J. Med. Chem.* **2008**, *51*, 5243-5263.

(17) Sherer, B. A.; Hull, K.; Green, O.; Basarab, G.; Hauck, S.; Hill, P.; Loch, J. T., 3rd; Mullen, G.; Bist, S.; Bryant, J.; Boriack-Sjodin, A.; Read, J.; DeGrace, N.; Uria-Nickelsen, M.;

Illingworth, R. N.; Eakin, A. E. Pyrrolamide DNA gyrase inhibitors: optimization of antibacterial activity and efficacy. *Bioorg. Med. Chem. Lett.* **2011**, *21*, 7416-7420.

(18) Basarab, G. S.; Hill, P. J.; Garner, C. E.; Hull, K.; Green, O.; Sherer, B. A.; Dangel, P. B.; Manchester, J. I.; Bist, S.; Hauck, S.; Zhou, F.; Uria-Nickelsen, M.; Illingworth, R.; Alm, R.; Rooney, M.; Eakin, A. E. Optimization of pyrrolamide topoisomerase II inhibitors toward identification of an antibacterial clinical candidate (AZD5099). *J. Med. Chem.* **2014**, *57*, 6060-6082.

(19) Tari, L. W.; Li, X.; Trzoss, M.; Bensen, D. C.; Chen, Z.; Lam, T.; Zhang, J.; Lee, S. J.; Hough, G.; Phillipson, D.; Akers-Rodriguez, S.; Cunningham, M. L.; Kwan, B. P.; Nelson, K. J.; Castellano, A.; Locke, J. B.; Brown-Driver, V.; Murphy, T. M.; Ong, V. S.; Pillar, C. M.; Shinabarger, D. L.; Nix, J.; Lightstone, F. C.; Wong, S. E.; Nguyen, T. B.; Shaw, K. J.; Finn, J. Tricyclic GyrB/ParE (TriBE) inhibitors: a new class of broad-spectrum dual-targeting antibacterial agents. *PLoS One* **2013**, *8*, e84409.

(20) Škedelj, V.; Tomašić, T.; Mašič, L. P.; Zega, A. ATP-binding site of bacterial enzymes as a target for antibacterial drug design. *J. Med. Chem.* **2011**, *54*, 915-929.

(21) Bisacchi, G. S.; Manchester, J. I. A new-class antibacterial—almost. Lessons in drug discovery and development: A critical analysis of more than 50 years of effort toward ATPase inhibitors of DNA gyrase and topoisomerase IV. *ACS Infect. Dis.* **2015**, *1*, 4-41.

(22) Hodnik, Ž.; Tomašić, T.; Mašič, L. P.; Chan, F.; Kirby, R. W.; Madge, D. J.; Kikelj, D. Novel state-dependent voltage-gated sodium channel modulators, based on marine alkaloids from *Agelas* sponges. *Eur. J. Med. Chem.* **2013**, *70*, 154-164.

(23) Tomašić, T.; Hartzoulakis, B.; Zidar, N.; Chan, F.; Kirby, R. W.; Madge, D. J.; Peigneur, S.; Tytgat, J.; Kikelj, D. Ligand- and structure-based virtual screening for clathrodin-derived human voltage-gated sodium channel modulators. *J. Chem. Inf. Model.* **2013**, *53*, 3223-3232.

(24) Zidar, N.; Jakopin, Ž.; Madge, D. J.; Chan, F.; Tytgat, J.; Peigneur, S.; Dolenc, M. S.; Tomašić, T.; Ilas, J.; Mašič, L. P.; Kikelj, D. Substituted 4-phenyl-2-aminoimidazoles and 4-phenyl-4,5-dihydro-2-aminoimidazoles as voltage-gated sodium channel modulators. *Eur. J. Med. Chem.* **2014**, *74*, 23-30.

(25) Peigneur, S.; Žula, A.; Zidar, N.; Chan-Porter, F.; Kirby, R.; Madge, D.; Ilaš, J.; Kikelj, D.; Tytgat, J. Action of clathrodin and analogues on voltage-gated sodium channels. *Mar. Drugs* **2014**, *12*, 2132-2143.

(26) Zidar, N.; Montalvao, S.; Hodnik, Ž.; Nawrot, D. A.; Žula, A.; Ilaš, J.; Kikelj, D.; Tammela, P.; Mašič, L. P. Antimicrobial activity of the marine alkaloids, clathrodin and oroidin, and their synthetic analogues. *Mar. Drugs* **2014**, *12*, 940-963.

(27) Hodnik, Ž.; Los, J. M.; Žula, A.; Zidar, N.; Jakopin, Ž.; Los, M.; Sollner Dolenc, M.; Ilaš, J.; Wegrzyn, G.; Peterlin Mašič, L.; Kikelj, D. Inhibition of biofilm formation by conformationally constrained indole-based analogues of the marine alkaloid oroidin. *Bioorg. Med. Chem. Lett.* **2014**, *24*, 2530-2534.

(28) Tomašič, T.; Nabergoj, D.; Vrbek, S.; Zidar, N.; Jakopin, Ž.; Žula, A.; Hodnik, Ž.; Jukič, M.; Anderluh, M.; Ilaš, J.; Sollner Dolenc, M.; Peluso, J.; Ubeaud-Séquier, G.; Muller, C. D.; Peterlin Mašič, L.; Kikelj, D. Analogues of marine alkaloids oroidin, clathrodin, and hymenidin induce apoptosis in human HepG2 and THP-1 cancer cells. *Med. Chem. Commun.* **2015**, *6*, 105-110.

(29) Brvar, M.; Perdih, A.; Renko, M.; Anderluh, G.; Turk, D.; Šolmajer, T. Structure-based discovery of substituted 4,5'-bithiazoles as novel DNA gyrase inhibitors. *J. Med. Chem.* **2012**, *55*, 6413-6426.

(30) Mayer, C.; Janin, Y. L. Non-quinolone inhibitors of bacterial type IIA topoisomerases: a feat of bioisosterism. *Chem. Rev.* **2014**, *114*, 2313-2342.

(31) PyMOL, Delano Scientific LLC, San Francisco, CA, http://pymol.sourceforge.net.

(32) Marinko, P.; Obreza, A.; Peterlin Mašič, L.; Krbavčič, A.; Kikelj, D. Synthesis of 2-amino-7,8-dihydro-6(5*H*)-quinazolinone, 2,4-diamino-7,8-dihydro-6(5*H*)-quinazolinone, 5,6,7,8-tetrahydro-2,6-quinazolinediamine and 5,6,7,8-tetrahydro-2,4,6-quinazolinetriamine derivatives. *J. Heterocycl. Chem.* **2000**, *37*, 405-409.

(33) Gilow, H. M.; Burton, D. E. Bromination and chlorination of pyrrole and some reactive 1-substituted pyrroles. *J. Org. Chem.* **1981**, *46*, 2221-2225.

(34) Johnson, F.; Paul, K. G.; Favara, D. An efficient synthesis of methyl Dl-*cis*-jasmonate. *J. Org. Chem.* **1982**, *47*, 4254-4255.

(35) Schneider, C. S.; Mierau, J. Dopamine autoreceptor agonists: resolution and pharmacological activity of 2,6-diaminotetrahydrobenzothiazole and an aminothiazole analogue of apomorphine. *J. Med. Chem.* **1987**, *30*, 494-498.

(36) Ranieri, B.; Robles, O.; Romo, D. Concise synthesis of the isothiourea organocatalysts homobenzotetramisole and derivatives. *J. Org. Chem.* **2013**, *78*, 6291-6296.

(37) Durrant, J. D.; de Oliveira, C. A.; McCammon, J. A. POVME: an algorithm for measuring binding-pocket volumes. *J. Mol. Graph. Model.* **2011**, *29*, 773-776.

(38) Lu, J.; Patel, S.; Sharma, N.; Soisson, S. M.; Kishii, R.; Takei, M.; Fukuda, Y.; Lumb, K. J.; Singh, S. B. Structures of kibdelomycin bound to *Staphylococcus aureus* GyrB and ParE showed a novel U-shaped binding mode. *ACS Chem. Biol.* **2014**, *9*, 2023-2031.

(39) Basarab, G. S.; Manchester, J. I.; Bist, S.; Boriack-Sjodin, P. A.; Dangel, B.; Illingworth, R.; Sherer, B. A.; Sriram, S.; Uria-Nickelsen, M.; Eakin, A. E. Fragment-to-hit-to-lead discovery of a novel pyridylurea scaffold of ATP competitive dual targeting type II topoisomerase inhibiting antibacterial agents. *J. Med. Chem.* **2013**, *56*, 8712-8735.

(40) Lafitte, D.; Lamour, V.; Tsvetkov, P. O.; Makarov, A. A.; Klich, M.; Deprez, P.; Moras, D.; Briand, C.; Gilli, R. DNA gyrase interaction with coumarin-based inhibitors: the role of the hydroxybenzoate isopentenyl moiety and the 5'-methyl group of the noviose. *Biochemistry* **2002**, *41*, 7217-7223.

(41) Rarey, M.; Kramer, B.; Lengauer, T.; Klebe, G. A fast flexible docking method using an incremental construction algorithm. *J. Mol. Biol.* **1996**, *261*, 470-489.

(42) Rarey, M.; Wefing, S.; Lengauer, T. Placement of medium-sized molecular fragments into active sites of proteins. *J. Comput. Aid. Mol. Des.* **1996**, *10*, 41-54.

(43) BioSolve IT (GmbH), LeadIT version 2.1.3.

(44) Alt, S.; Mitchenall, L. A.; Maxwell, A.; Heide, L. Inhibition of DNA gyrase and DNA topoisomerase IV of *Staphylococcus aureus* and *Escherichia coli* by aminocoumarin antibiotics. *J. Antimicrob. Chemother*. **2011**, *66*, 2061-2069.

(45) GAMESS interface, ChemBio3D Ultra 13.0, ChemBioOffice Ultra 13.0, CambridgeSoft.

(46) Halgren, T. A. Merck molecular force field .1. Basis, form, scope, parameterization, and performance of MMFF94. *J. Comput. Chem.* **1996**, *17*, 490-519.

(47) Baell, J. B.; Holloway, G. A. New substructure filters for removal of pan assay interference compounds (PAINS) from screening libraries and for their exclusion in bioassays. *J. Med. Chem.* **2010**, *53*, 2719-2740.

Table of contents graphic